Acta Mechatronica - International Scientific Journal about Mechatronics
Volume: 1 2016 Issue: 2 Pages: 1-5 ISSN 2453-7306

MEASURING OF YOUNG'S MODULUS OF THIN SAMPLES USING THE QUICK BENDING VIBRATIONS OF SEARLE'S PENDULUM

Karol Kvetan
Slovak University of Technology, Faculty of Materials Science and Technology, Institute of Materials Science, Bottova 25, 917 24 Trnava, Slovak Republic, karol.kvetan@stuba.sk
Martin Bučány
Slovak University of Technology, Faculty of Materials Science and Technology, Institute of Materials Science, Bottova 25, 917 24 Trnava, Slovak Republic, xbucany@stuba.sk
Ondrej Bošák
Slovak University of Technology, Faculty of Materials Science and Technology, Institute of Materials Science, Bottova 25, 917 24 Trnava, Slovak Republic, ondrej.bošák@stuba.sk
Marián Kubliha
Slovak University of Technology, Faculty of Civil Engineering, Radlinského 11, 810 05 Bratislava, Slovak Republic, marian.kubliha@stuba.sk
Janette Kotianová
Slovak University of Technology, Faculty of Materials Science and Technology, Institute of Applied Informatics, Automation and Mechatronics, Bottova 25, 917 24 Trnava, Slovak Republic, janette.kotianova@stuba.sk

Keywords: Young's modulus, Searle's pendulum, quick bending vibrations, step procedure
Abstract: In this paper we present accurate measurements of elastic modulus of thin quick-vibrating wire samples by Searle´s pendulum. We provide detailed statistical analysis of measurement of one "non-traditional" sample - with a rectangular cross-section. In our paper we present the measurement of Young's modulus at quick-vibrating samples where vibrations are registered and analysed by electronic sensor or camera. Also, other necessary instruments (micrometre, calibre, weight) were on an electronic basis, which was a guarantee of high accuracy measurements. The degree of an accuracy being achieved was subjected by a detailed theoretical analysis, using knowledge of theory of the uncertainties.

1 Introduction

Elastic modulus (also called tensile modulus or Young's modulus) E belongs to the most important material constants. It determines the relation between mechanical stress σ along the axis, and strain ε at axial loading, in the form $\sigma = E\varepsilon$, which is valid in the range of Hooke's law. Higher loading of the sample may result in exceeding the limits of elastic behaviour of the material.

There exist several ways for measuring this quantity. The best know methods are as follows: mechanical (static and dynamic), acoustic, ultrasonic, resonant, optical, etc. Mechanical methods are the most suitable for measuring elastic modulus E of thin samples, such as rods, wires, columns, fibres, etc. Application of the static methods (e.g. direct prolongation, two- and three- point bending etc.) however, is rather disadvantageous, as they can hardly reach accuracy better than 10 % [1].

Greater accuracy can be achieved using dynamic methods. Elastic modulus E can be determined with several per cent accuracy by means of vibrating samples at single - or three-point bending [2], or by balance of apparatus so called as Searle´s pendulum [3], [4].

In the case of pendulum device it is, however, a disadvantage that this procedure can only be used for thin samples of wire or fibre form. Additionally, using standard optical techniques (that is monitored and accounted oscillations by the eye), the area of useful samples would be further reduced to the set in which the vibration movement is relatively slow, and such the counting of oscillations is manageable "by the naked eyes".

In our paper we present the measurement of Young's modulus at quick-vibrating samples where vibrations are registered and analysed by electronic sensor or camera. Also, other necessary instruments (micrometre, calibre, weight) were on an electronic basis, which was a guarantee of high accuracy measurements. The degree of an accuracy being achieved was subjected by a detailed theoretical analysis, using knowledge of theory of the uncertainties.

2 Description of measurement

Dynamic method of measuring the modulus of elasticity with usually used bending oscillations in

Acta Mechatronica - International Scientific Journal about Mechatronics
Volume: 1 2016 Issue: 2 Pages: 1-5 ISSN 2453-7306

MEASURING OF YOUNG'S MODULUS OF THIN SAMPLES USING THE QUICK BENDING VIBRATIONS OF SEARLE'S PENDULUM

Karol Kvetan; Martin Bučány; Ondrej Bošák; Marián Kubliha; Janette Kotianová

single- or three- point bend brings one disadvantage: the oscillations are too fast, and therefore difficult to measure.

The situation would be simpler if we should reduce their frequency somehow.

2.1 Searle's pendulum

One such method has been invented by American physicist G.F.C Searle [3], [4]. He suggested a simple idea - to attach the ends of the measuring sample to the flywheel housings. These subjects "remove from the powder" a part of their vibratory mechanical energy and thus significantly slow down the process to the level of electronically readable, sometimes even to the naked eye.

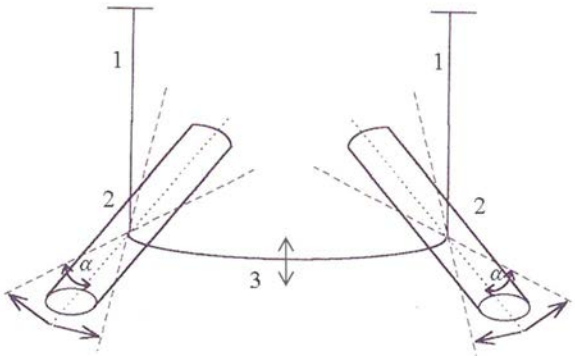

Figure 1 Searle´s pendulum.
1 – hanging threads, 2 – cylinder flywheels, 3– measured wire (arrows indicate the direction of the oscillations)

Such a device - known as Searle's pendulum - it is suitable for measuring samples with a small cross section. It consists of three main parts (Figure 1): between two hinge yarns 1 are fixed horizontally the flywheels (cylindrical or prismatic) 2, they are connected by the measured sample 3; this one basically represents the element of "coupling". Usually it is in the form of wire, but it can also be a thin rod, thread or thin prismatic tape. Symmetrical deflection of the flywheels in the horizontal direction by the angle α performs the bending oscillating movement of the sample that is reversely transmitted to the oscillating rotary motion of flywheels - and vice versa. Both parts of a pendulum – i.e. flywheels and sample - oscillate synchronously, with the same frequency and phase.

For information – such apparatus in miniature form is currently used in textile industry for examination of the elasticity of fibres, or in botany for the analogous research of plant stalks.

Dynamic analysis of the process [2], [3] gives for the measured modulus E of routinely used samples with circular cross-section, a final relationship

$$E = \frac{8\pi lJ}{r^4 T^2} \qquad (1)$$

wherein l is the length of the sample with the radius r. T means the oscillation period of the system, and J is the moment of inertia of the flywheel with respect to the perpendicular axis passing through the centre (this is the same as the direction of the hinge yarns). For the less used samples with a rectangular cross-section it is [2]

$$E = \frac{24\pi^2 lJ}{a^3 b T^2} \qquad (2)$$

where a and b are the width and height of the sample (this is the flywheels detained in height direction, i.e. in the direction in which bending vibrations are possible).

But now we must differentiate the type of flywheels, too. In the case of cylindrical flywheels, as well as in our picture, the moment of inertia is given by the known relationship

$$J = m\left(\frac{L^2}{12} + \frac{R^2}{4}\right) \qquad (3)$$

The parameters R and L are the diameter and length of flywheels, and m means their (single) mass. In the case of square flywheels it would be

$$J = \frac{1}{12} m(A^2 + B^2) \qquad (4)$$

wherein A and B are the length and the width of the prism.

2.2 *The experimental assembly for measurement*

We used the illustrated apparatus (Figure 2). It consist of two homogeneous steel rollers in the role of flywheels, each having a mass m = 0,72 kg, a length L = 137 mm and a radius r = 14,6 mm. Size of moment of inertia of each of them, determined from the relation (3), had a value of J = 1,15 x 10^{-3} kg.m^2. We performed measurements of several samples of wires with circular cross section and one of them with rectangular section. All the samples had the same "active" length (i.e. the distance between the points of attachment to flywheels) l = 0,295 m.

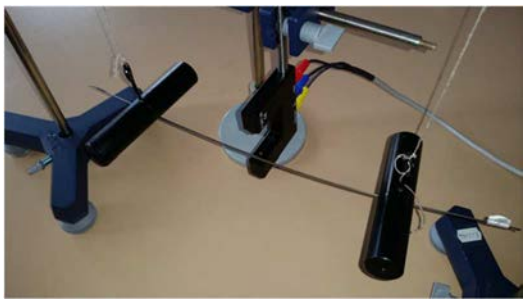

Figure 2 Experimental assembly. Vibrating wire sample crosses the infrared beam of an optical sensor (prismatic body with the shape of figure U in the centre of operation)

Acta Mechatronica - International Scientific Journal about Mechatronics
Volume: 1 2016 Issue: 2 Pages: 1-5 ISSN 2453-7306

3 Results of measurements

Main parameters of the samples and results of measurements, including the cross-sectional geometrical dimensions, oscillation periods, together with the values of elasticity modulus are summarized below (Table 1).

Table 1 Parameters of samples and the results of measurements

Sample	Period of oscillation T (s)	Modulus of elasticity (measured) E_{meas} (GPa)	Table valued parameter E_{tab} (GPa)
Steel I – circle r = 1,00 mm	0,209	194,5	200 ± 10%
Steel II – circle r = 1,22 mm	0,138	201,5	200 ± 10%
Steel III – circle r = 1,25 mm	0,129	210,1	200 ± 10%
Copper – circle r = 1,00 mm	0,271	116,3	115 ± 10%
Aluminium – circle r = 1,00 mm	0,355	67,4	70 ± 10%
Brass – circle r = 1,70 mm	0,099	104,7	95 ± 10%
Steel – rectangular a x b = (0,79 x 2,50) mm	0,596	185,6	200 ± 10%

E modules have been obtained using equation (1) and (2). We can see that the measured values E_{meas} correspond to the table ones E_{tab}, in all cases they are lying within the corresponding intervals. (We recall a known technological fact that the existence of these relatively "wide" intervals is related to factors such as different methods of preparation, types and quantities of used ingredients, etc.). We also see that all vibrations were relatively quick - with periods of the order of tenths of a second - so that we can benefit fully the advantages our measuring apparatus, e.g. the opportunity to electronically capture the rapid oscillations.

In the next section we shall carry on a detailed analysis of the results of the steel wire sample with rarely occurring rectangular cross section with dimensions of 0,79 mm x 2,50 mm; in other words – with geometry of a sort of certain "prismatic strip". This measurement has been executed by stepwise procedure – i.e. by the method commonly used in the pendulum experiments. Finally, we had determined the percentage uncertainty in the results.

We performed measurements of 100 oscillation acts. As it is known, a stepwise procedure is the method in which we record the splits, in this case every 10 strokes.

Table 2. Results of measuring of the vibrations by stepwise procedure. The first and the third columns give the number of oscillations, the second and the fourth columns reflect the relevant times. The fifth column presents the difference of them, and corresponds to the time of 50 oscillations

i_I	$T_{i_I}(s)$	i_{II}	$T_{i_{II}}(s)$	$T_{i_{II}} - T_{i_I} = T_{i_{50}}(s)$	$\Delta T_{i_{50}} = T_{i_{50}} - \bar{T}_{50}(s)$	$(\Delta T_i)^2(s^2)$
10	5,965	60	35,790	29,825	-0,001	0,000 001
20	11,925	70	41,755	29,830	+0,004	0,000 016
30	17,895	80	47,725	29,835	+0,004	0,000 016
40	23,860	90	53,685	29,825	-0,001	0,000 001
50	29,830	100	59,650	29,820	-0,006	0,000 036
				$\bar{T}_{50} = 29{,}826$ s		$\sum(\Delta T_i)^2 = 0{,}000\,070\ s^2$

The results will be listed in the table (Table 2) into two columns: the first one represents the first part of the measurement, i.e. range of 0 - 50 oscillations, the other corresponds to the second part from 60 to 100 strokes. We will do the differences of both of them and record it to the third column; so we get 5 different values corresponding to 50 oscillations. These results can be evaluated statistically (see last two columns + additional

Acta Mechatronica - International Scientific Journal about Mechatronics
Volume: 1 2016 Issue: 2 Pages: 1-5 ISSN 2453-7306

MEASURING OF YOUNG'S MODULUS OF THIN SAMPLES USING THE QUICK BENDING VIBRATIONS OF SEARLE'S PENDULUM

Karol Kvetan; Martin Bučány; Ondrej Bošák; Marián Kubliha; Janette Kotianová

calculations). "Philosophical" principle of this method - opposite of the method of arithmetic average - lies in the fact, that the single measurement of 100 oscillations will be replaced by five 50-wobble measurements. Statistical evaluation applied here would be more precise and the resulting uncertainty would be lower, too.

We had received an average value for one period $\overline{T} = \frac{\overline{T}_{50}}{50} = 0{,}596$.

The corresponding uncertainty can be derived as in the case of physical quantity being measured by the direct route $u_T = \pm\frac{1}{50}\sqrt{\frac{\Sigma(\overline{T}-T_i)^2}{n(n-1)}} = 0{,}000037\ s$, wherein n = 5 means the number of measurements. This number can be considered as the size of the uncertainty of type A, too. It is clear that this value is too small for noticeable evaluating of overall uncertainty of u_E. Even if we should consider the impact of uncertainty of type B, that may be represented by the accuracy of the device in the order of five thousandths of a second, and the total time uncertainty we took as a sum of them, it will be - as we shall see later - still too little value to be strongly reflected (see calculation of overall uncertainty according to equation (5)).

We get for measuring modulus of elasticity (2) $E = \frac{24\pi^{2,296,3}.10^{-3}m.1{,}148.10^{-3}kg.m^2}{(0{,}79.10^{-3}m)^{3.2,50}.10^{-3}m.(0{,}593s)^2} = 185{,}64$.

Evaluation of the corresponding uncertainty that it will be a little lengthier. Here we must consider that the determination of the modulus of elasticity - as can be seen from equation (2) – is a function of five variables x_i; namely $E = f(I, J, a, b, T)$. In this case – in accordance with theory of measurements - the uncertainty is given by a root, containing partial derivatives with respect to all of the relevant variables and uncertainties of the following variables:

$$u_E = \sqrt{\sum_{i=1}^{n}\left(\frac{\partial E}{\partial x_i}u_{x_i}\right)^2} = \sqrt{\left(\frac{\partial E}{\partial l}u_l\right)^2 + \left(\frac{\partial E}{\partial J}u_J\right)^2 + \left(\frac{\partial E}{\partial a}u_a\right)^2 + \left(\frac{\partial E}{\partial b}u_b\right)^2 + \left(\frac{\partial E}{\partial T}u_T\right)^2} \quad (5)$$

The relevant partial derivatives are

$$\frac{\partial E}{\partial l} = \frac{\partial\frac{24\pi^2 lJ}{a^3bT^2}}{\partial l} = \frac{24\pi^2 J}{a^3bT^2}$$
$$\frac{\partial E}{\partial J} = \frac{\partial\frac{24\pi^2 lJ}{a^3bT^2}}{\partial J} = \frac{24\pi^2 l}{a^3bT^2}$$
$$\frac{\partial E}{\partial a} = \frac{\partial\frac{24\pi^2 lJ}{a^3bT^2}}{\partial a} = -\frac{72\pi^2 lJ}{a^4bT^2}$$
$$\frac{\partial E}{\partial b} = \frac{\partial\frac{24\pi^2 lJ}{a^3bT^2}}{\partial b} = -\frac{24\pi^2 lJ}{a^3b^2T^2}$$
$$\frac{\partial E}{\partial T} = \frac{\partial\frac{24\pi^2 lJ}{a^3bT^2}}{\partial T} = -\frac{48\pi^2 lJ}{a^3bT^3} \quad (6)$$

It is necessary to clarify the uncertainty of the moment of inertia u_J (7). This quantity has been not measured directly, but - as seen from the equation (3) – it is a function of the directly measured quantities *M*, *L*, *R*, and its uncertainty must therefore also be determined by means of the partial derivatives:

$$u_J = \sqrt{\left(\frac{\partial J}{\partial m}.u_m\right)^2 + \left(\frac{\partial J}{\partial L}.u_L\right)^2 + \left(\frac{\partial J}{\partial R}.u_R\right)^2},$$

e.g.

$$u_J = \sqrt{\left(\left(\frac{L^2}{12}+\frac{R^2}{4}\right)\cdot u_m\right)^2 + \left(m\frac{L}{6}\cdot u_L\right)^2 + \left(m\frac{R}{2}\cdot u_R\right)^2} \quad (7)$$

For a determination the uncertainty of time we have established an uncertainty of type B, referred above, i.e. u_t = 0,005 s. Other quantities measured by direct route (flywheel length *L*, its radius *R* and mass *m*, length samples *l* and the cross-sectional dimensions *a* and *b*) had been measured once time, only; therefore we felt the precision of measuring instruments for applying the uncertainties of them as the size of the smallest pieces on their scales. So:

u_L = 0,1 mm (sliding ruler)
u_r = 0,01 mm (micrometer)
u_l = 1 mm (ruler)
u_a, u_b = 0,01 mm (micrometer)
u_m = 1 g = 0,001 kg (laboratory scales).

Substituting into (6) gives a value of u_J = 1,5 x 10^{-5} kg.m^2. As we can see after further substituting into (5) the last three members in the roof are some orders of magnitude smaller than the previous two members, so that we can neglect them. It recognizes the value of a numerical expression of uncertainty u_E = 5,94 GPa, which represents about 3,2% against the size of the module being measured.

So, the final result can be written as E = (185,64 ± 5,94) GPa, resp. E = 185,64 GPa ± 3,2 % .

The value of total uncertainty is given by the sum of partial uncertainties of types A and B. As we know from the theory of measurement, the causes of uncertainty A are unknown. However, the causes of uncertainty B it is not difficult to determine, they related with an accuracy of instruments, uncertainty in the readings and air resistance against the vibrating motion. Other factors, such as a non-

MEASURING OF YOUNG'S MODULUS OF THIN SAMPLES USING THE QUICK BENDING VIBRATIONS OF SEARLE'S PENDULUM

Karol Kvetan; Martin Bučány; Ondrej Bošák; Marián Kubliha; Janette Kotianová

uniformity of wire thickness, directional moment of the hanging threads, heating the samples as a result of oscillations etc. are negligible.

Note: Searle's pendulum can be used - after small adjustments - as a torsion pendulum, too. It will suffice to remove the hanging threads and one of flywheels let it hang freely at the end of the measured wire. After being displaced, the flywheel will be performing the horizontal oscillations due to torsional forces of wire (Figure 3).

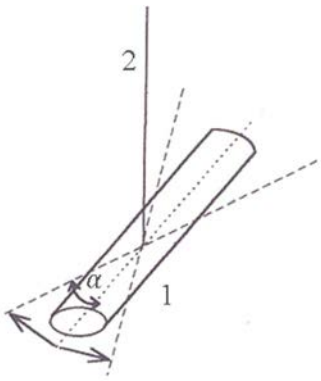

Figure 3 Flywheel (1) of Searle's pendulum hanging on wire sample (2) used as a torsion pendulum

By this way it is possible to determine the shear modulus G (8) as [4]

$$G = \frac{8\pi l J}{r^4 T_G^2} \qquad (8).$$

This relationship is substantially identical with an equation (1), but the oscillation period T_G of Young's modulus in the denominator is replaced by torsion oscillation period T_G.

Using known values of E and G it is possible to determine a next important material constant – the Poisson's number μ (9) as

$$\mu = \frac{E}{2G} - 1 \qquad (9).$$

The measurement of these parameters, however, has not been a filling of our work.

Conclusion

Searle's pendulum, though a simple and fairly accurate device to measure elastic modulus, is used relatively few (unfairly in our opinion). Additionally, it should be mostly in the cases of "slow oscillating" samples of circular cross section. Either as the applications in textile industry and in botany, mentioned above, is rather exceptional.

Some benefit of our paper is the fact that we performed measurements with "non-traditional" rectangular pattern. Other priority is related to higher degree of precision being achieved - because of the time was measured by an electronic detector or fast camera, respectively. This was reflected in a small error of measuring (3,2%) and in the fact that all the values.

In the near future we plan to extend the measurement on inhomogeneous samples, for example to examine how the surface coating will affect their module.

Acknowledgment

The article was created within framework of the projects KEGA No.001STU-4/2014 „Implementation of non-destructive methods for investigation of physical properties of progressive thin-layer methods“ (Slovak Republic).

References

[1] ŠTUBŇA, I., KOZÍK, T.: Factors affecting the accuracy of the measurement elastic modulus and mechanical strength, *Sklář a keramik*, No.8, pp. 228-230, 1979.

[2] TIMOSHENKO S., YOUNG D. H., WEAWER W.: *Vibration Problems in Engineering*, John Wiley and Sons, New York, 1974.

[3] BRAWN, R.: *General Properties of Matter*, London, Butherwords, 1969.

[4] FRIŠ, S.E., TIMOREVA, A.V.: *Kurz fysiky I*, NČSAV, 1957 (Original in Slovak).

Review process

Single-blind peer reviewed process by two reviewers.

Acta Mechatronica - International Scientific Journal about Mechatronics
Volume: 1 2016 Issue: 2 Pages: 7-13 ISSN 2453-7306

MACHINE VISION INVESTIGATE THE TRAJECTORY OF THE MOTION HUMAN BODY- REVIEW OF THE METHODS

Piotr Kuryło
University of Zielona Góra, Faculty of Mechanical Engineering, Institute of Machine Bulding and Exploatation, Zielona Gora, Poland, p.kurylo@ibem.uz.zgora.pl
Joanna Cyganiuk
University of Zielona Góra, Faculty of Mechanical Engineering, Institute of Machine Bulding and Exploatation, Zielona Gora, Poland, j.cyganiuk@ibem.uz.zgora.pl
Edward Tertel
University of Zielona Góra, Faculty of Mechanical Engineering, Institute of Machine Bulding and Exploatation, Zielona Gora, Poland, e.tertel@ibem.uz.zgora.pl
Peter Frankovský
Technical University of Košice, Department of Applied Mechanics and Mechatronics, Košice, Slovak Republic, peter.frankovsky@tuke.sk

Keywords: machine vision, rehabilitation, dedicated software, lighting
Abstract: The paper presents the analysis of possible applications of vision appliances in the measurements of motion trajectory of a limb (or all body) mainly in rehabilitation exercises. The paper also presents the analysis of techniques of carrying out measurements of trajectories of particular limbs including issues concerning: correct lighting of the studied object, marker selection as well as selection of image recording appliences. The paper also discusses the basic components of the vision systems designed for the limb motion registering as well as possible applications of the systems in the object (patient) identification. Exemplary applications of the systems for measurement of a trajectory of upper limbs motion have been also presented. The paper also discusses extensively the SFRT system designed for measuring and recording the motion range in human joints as well as a method of recording the results of measurements with the use of the SFRT technique depending on the kind of a joint.

1 Introduction

Machine vision systems usually enclose a camera and a machine analysing images, for example a computer with suitable software. All subsystems must be selected appropriately to needs of the determined application, in addition the problem of using the image processor in order to provide a proper time of acting and a suitable resolution of the system of imaging is crucial here [1], [3], [4], [7], [14].

Machine vision systems are used in non-invasive and non-impact measurements. These systems are used in the production as tools supporting the quality control, control of measurement of the geometry of the product, etc. in view to their character; they are also applied in medicine [1], [3], [8], [10-11], [15], [17], [23]. At present, the major attention is focused on registering the movement of a human body in form of a sequence of images [16], [18], [21], [23]. The main problem connected with the motion of a human figure is in estimating of the current configuration of the human silhouette. It is one of most difficult problems in the computer image processing, especially in view of a big space of research, diversity of human figures and environments of the observed individual. Works on observing the motion of the human body usually use simplified models [18],[24], homogenous environment [16] and properly selected clothes for the human body, in order to determine its characteristics. In the work [16] there has been created a system for observing movements of man, based on a geometric, three-dimensional model. The system was using images from three calibrate cameras. Experiments were realized in scenarios with black background. Although, there was used an improved molecular filter with the algorithm of the simulated event, still obtained periods of calculations were very long. Systems built from many cameras (so-called multi-cameras systems) [16], [20], [21] are usually used in applications observing movements of human individuals in order to obtain better results in the context of mutual hiding from view by human limbs and elements of the body. Applications of this type usually use probabilistic models of human silhouette [21] or its three-dimensional models [16], [18], [19], [24].

The application of a modern machine vision system might another method for analysing movements and modelling the motion and the figure of man.

The motion analysis encloses three parts: kinematics, kinesiological, electromyography and kinetics.

Kinesiological should be understood as a set of diagnostic procedures used in establishing the course of the rehabilitation with the physiotherapist; it constitutes a

Volume: 1 2016 Issue: 2 Pages: 7-13 ISSN 2453-7306

basis for preparing a plan of the therapy (long or short term) in order to resolve the problem of the patient.

It consists in gathering current information on patient's ailments, on his work environment, on sports he practices, on his household, in order to reduce its movement efficiently because the motion is the reason presented problems. The next part of the interview, enclosed in the procedure, consists in collecting information on the history of patients' diseases, injuries and operations he had during his life, or even some pieces of information not related with his current condition.

Kinesiological procedures enclose also studying muscles, valuing the mobility of joints and measurement of its level, examination of chosen functions for each area of the locomotive system – so called motional stereotypes.

Conclusions from Kinesiological can facilitate establishing suitable equipment for the rehabilitation. They can also help in getting additional information necessary in the further, additional diagnostics and methods of obtaining images, like RTG and USG.

From the point of view of technological solutions, modern systems for motion analysis can be classified into following groups [1],[5],[8], [10], [17]:

systems based on the digitization of images obtained from few video cameras (at least two),

systems based on the identification of markers placed on the body of the examined person:

- systems based on active markers,
- systems based on passive markers,
- ultrasonic systems.

All systems for motion analysis enclose also software for activation and preliminary processing of obtained data and software for preparing results of measurements and preparing reports, as well as specialist programs for creating biomechanical models.

All methods of measurement used in the objective, quantitative analysis of movement, can be divided into three groups [2], [4], [9], [15]:

- first group, which measure parameters of time and spacer (the tempo of walk, the frequency of steps, the length of steps, participation of individual phases in the cycle of walk or run, etc. In other words – the cycle of periodical motions).
- second group encloses kinematic methods that measure the trajectory of the motion in chosen points of the body, which is examined in a three dimensional space, as well as a (direct or indirect) measurement of angles in joints, determining the sense of direction of individual segments of the body towards oneself and measuring the speed and accelerations of one section of the body relative to the adjacent section.
- third group encloses kinetic methods measuring (directly or indirectly) forces and moments of forces that occur during the process of movement.

All systems for motion analysis can be integrated with other equipment and they can synchronize the register of data from all of them:

- systems for the surface electromyography,
- dynamographic platform,
- microswitches.

Systems based on active and passive markers also enable additional integration with one or two cameras recording the course of the examination, which are synchronized with vision data.

2 Systems for motion analysis criteria in clinical applications

Systems for motion analysis can be applied in ergonomic or sport studies, in film studios and in clinical examinations. Systems applicable in clinics should be characterized with following criteria [2], [9], [14], [25], [26]:

- a relatively big space of measurement that allows the patient to "fan out": kinematic and speed parameters stabilize only after the 2/3 of the step; the register should enclose the entire cycle of the left foot step forward and the right foot step forward; this means that the length of the measurement space should be : (3 x 65 cm = 2 m – "fan out" steps) + (2 x 1 m = 2 m – two cycles of walk) + (2 m – additional distance from cameras) = 6 m;
- small measuring vagueness (less than 1 mm),
- a relatively simple marker that requires not many markers (especially in case of small children), which will not make the cooperation with other systems difficult (for example for the dynamic electromyography),
- records made in c3d format,
- a relatively user friendly and simple software for activation and processing data with simultaneous provision of flexibility, which is necessary in scientific research,
- possibility of integrating and synchronizing the system with other measurement systems (microswitches, dynamographic platforms, dynamic electromyography systems) and integrating them in the software and c3d files.

Different systems, depending on their types, producer and model, have varied accuracy. More detailed information on the accuracy of different system is presented below.

The majority of systems for motion analysis using the digitalization of the video image in the course of three-dimension reconstruction obtain a measurement with a degree of inaccuracy equal 5.4 mm (± 2.7 mm) in the sagittal plain and 3.8 mm (± 1.9 mm) in the frontal plane and 6.0 mm (± 3.0 mm) in the transverse plane. This inaccuracy is not characteristic for all systems. For example, the Ariel APAS system has more inaccuracy,

Volume: 1 2016 Issue: 2 Pages: 7-13 ISSN 2453-7306

equal circa 11.6 mm [12], and the Dynas system reaches even up to 18.42 mm.

In case of the optoelectronic system VICON 370 the inaccuracy of measurement of the centre of the marker is determined on the level of 2 mm with the assumed distance of 500 mm between markers with the diameter of 25 mm. reducing the diameter of markers to 14 mm allows obtaining the accuracy of less than 1 mm, i.e. 0.98 mm. Lately, after the implementation of the new generation of MX cameras, and even T cameras, according to information of the producer, the inaccuracy of the measurement dropped significantly and now it reaches the scale of less than 0.05 mm.

Designed vision systems allow among other [9], [25], [26]:

- optical motion analysis of the limb, but also an optical motion analysis of any part of the body (limbs, palms, but also the spine),
- the result of the analysis is explicit and does not require additional processing and analyses,
- the system allows making examinations in conditions of illumination typical for medical rooms and rooms, in which the rehabilitation is being conducted,
- the designed system guarantees the possibility of diversifying markers overlapping each other, removing and correcting system errors, creating and deleting new points, changing names assigned to markers. Changes can be conducted in the 2-D vision and in the X-Y system of coordinates.

It is worth underlining that every producer of systems for motion analysis guarantees fundamental software for activating and preliminary processing data.

Defining software for activation and preliminary processing data in a determined vision system gives possibilities as follows [26]:

- it allows sizing the system (i.e. determining the position and orientation of cameras in view to the global system of coordinates) before the initiating the data collecting,
- simultaneous gathering vision data and analogical data,
- synchronization in time of all gathered data,
- creating a fundamental database, in which data from examinations is being collected.

In case of systems based on the digitalization of the video image, the software additionally allows automation of marking characteristic points of the patient's body in following action shots.

In case of marker systems, it allows supplementing gaps in trajectories of markers and filtering data.

Depending on the producer, further stages of the data is processing and analysis can be realized in different ways.

Some producers use the software from external companies, which make the further data processing, i.e. forming a model on basis of localizations of markers in the local system of coordinates, they calculate angles in individual joints and they send obtained data to the final report. The Visual 3D software, produced by C-Motion company is the most popular program. It is used among other by companies like Qualisys or Charnwood Dynamics.

Data collected with use of these systems for motion analysis constitute the basis for making biomechanical models.

Biomechanical models can have following purposes [1], [5], [8], [20]:

- estimating charges during motor tasks of different kind impossible for the direct measurement (like in joints),
- estimating charges of the body while acting of different powers and outside moments (collisions, injuries),
- estimating the disintegration of muscle forces during various motor tasks in the norm and in pathology,
- estimating the changes of length of muscles.

Most popular software programs are:

- Anybody (www.anybodytech.com),
- SIMM (Software for Interactive Musculoskeletal Modeling) (www.msculographics.com),
- OpenSim –Open Source (smtk.org) type of software.

It is known that the rehabilitation is aimed at giving back the lost ability to the patient, initiating actions for preventing the occurrence of such disability, as well as precipitating producing substitute compensating mechanisms – in case of morphological permanent damages.

The efficiency of rehabilitation for people with disabilities can be improved by the application of manipulators or rehabilitation robots (for therapy, physiotherapy). Therefore, the rehabilitation robotics is a domain that focuses on using manipulators and robots in the rehabilitation of people with disabilities.

The use of Internet enables the development of a new method of rehabilitation of disable people called telerehabilitation.

In order to establish the degree of the progress of illness, determining the degree of the malfunction of the pathologically changed limb, a range of measurement must be made. The measurement of movement in joints is made with special instruments called goniometers. In past years, a SFTR method is achieving popularity. It is a method of measuring particular movements in particular planes: Sagittal-S, Frontal-F, Transverse-T and Rotation-R and recording results. The use of this method aims at increasing the objectivism of measurement of ranges of motions. Movements in all joints are measured from the initial position – a so-called neutral zero, and all positions and movements are described in all of three dimensions mentioned before - SFTR [5].

Coupling the vision machine system with the SFTR method resulted with the occurrence of a new diagnostic, non-invasive, measuring method.

MACHINE VISION INVESTIGATE THE TRAJECTORY OF THE MOTION HUMAN BODY- REVIEW OF THE METHODS

Piotr Kuryło; Joanna Cyganiuk; Edward Tertel; Peter Frankovský

The Table 1.1.is illustrating an exemplary record of angle measurement for a human joint obtained with use of the SFTR method.

The record is coherent with requirements of ISOM (International Standard Orthopaedic Measurements) standards.

Table 1.1. Record of the SFTR system of measurements of angles in human joints in accordance with ISOM (International Standard Orthopaedic Measurements) standards – joints: cervical, thoracic, spine and the cingula of upper and lower limbs [5]

Joints	SYMBOL OF THE PLANE	Movements	Standard of ISOM
Of cervical spine	S	Extention-0-bend	40-0-40
	F	Side bend -0- Side bend Left right	45-0-45
	R	Rotation left – 0- rotation right	50-0-50
Of thoracic and lumbar spine	S	Extention-0-bend	30-0-85
	F	Side bend -0- side bend Left right	30-0-30
	R	Rotation left – 0- rotation right	45-0-45
Of the cingule of upper and lower limbs	S	Extention-0-bend	50-0-170
	F	abduction –0- adduction	170-0-0
	T	Extention Bend horisontally	30-0-135
	R	rotation – 0 – rotation inside outside	R(F0)* 60-0-70
		rotation – 0 – rotation outide inside	R(F90) 90-0-80

A correct assortment of the illumination is an important problem in creating the vision machine system. It is one of most important operation in the course of preparing the vision system for work. A proper illumination provides an image with correct parameters, which in turn guarantee the required functioning of the entire system. The illumination of the object often changes depending on extrinsic factors (movement of the sun, changing illumination) and, in consequences, causes problems in the correct functioning of the system. Therefore, very often an additional source of light, dedicated to the system and independent from external factors, is used in the examination. The choice of illumination is determined by many factors and at the end, for every system, this parameter is individually adjusted [29-30], [33].

Table 1.1,. 1.2, 1.3 and 1.4 presents record of the SFTR system of measurements of angles in human joints.

Table 1.2. Record of the SFTR system of measurements of angles in human joints in accordance with ISOM (International Standard Orthopaedic Measurements) standards – joints: elbow, prearm, radiocarpal, wrist, [5]

Joints	SYMBOL OF THE PLANE	Movements	Standard of ISOM
Elbow	S	Extention – 0 - bend	0-0-150
Prearm	R	Supination – 0 - pronation	90-0-80
Radiocarpal and wrist	S	Extention-0-bend	50-0-60
	F	abduction abduction radial -0- elbow	20-0-30

Table 1.3. Record of the SFTR system of measurements of angles in human joints in accordance with ISOM (International Standard Orthopaedic Measurements) standards – joints: carpal and metacarpal 1, metacarpophalangeal 1, metacarpophalangeal 2-4, proximal interphalangeal 2-4, distal interphalangeal 2-4 [5]

Joints	SYMBOL OF THE PLANE	Movements	Standard of ISOM
Carpal and metacarpal 1	VF	Extention-0-bend	30-0-15
	VS	abduction -0- adduction	40-0-0
	CR	lead-0-abduction	20-0-90
metacarpo phalangeal 1	S	Extention-0-bend	5-0-50
metacarpo phalangeal 2-4	S	Extention-0-bend	30-0-90 Variable
	F	abduction-0-adduction	
metacarpo phalangeal 1	S	Extention-0-bend	15-0-05
proximal interphalangeal 2-4	S	Extention-0-bend	0-0-100
distal interphalangeal 2-4	S	extension -0- bend	0-0-80

MACHINE VISION INVESTIGATE THE TRAJECTORY OF THE MOTION HUMAN BODY- REVIEW OF THE METHODS

Piotr Kuryło; Joanna Cyganiuk; Edward Tertel; Peter Frankovský

The explanation of symbols included in Tables 1.1., 1.2., 13. And 1.4 is as follow:

- S- sagital plane; F- frontal plane; T- transverse plane; R- rotation plane
- *R(F0) – means in this case that the external and internal rotation of the shoulder are measured in a situation, in which the joint is in the frontal plane, placed in the adduction - F0*. R(F90) – this record means that both rotations are examined in position of the shoulder abducted are 90°.
- **(S90) – means that during the examination of movements of the rotation in the hip joint the knee joint is bent to 90°.
- ***(S0) – means that during the examination of movements of the rotation in the hip joint the knee joint is erect.

Table 1.4. Record of the SFTR system of measurements of angles in human joints in accordance with ISOM (International Standard Orthopaedic Measurements) standards – joints: coxal, knee, crurotalar articulation and Chopart's joints[5]

Joints	SYMBOL OF THE PLANE	Movements	Standard of ISOM
Coxal	S	Extention-0-bend	15-0-125
	F	abduction –0-adduction	45-0-25
	R	rotation – 0 – rotation	(S90)**
		outside	45-0-45
		inside	
	R	Rotation -0-rotation	(S0)***
		outside	
		inside	45-0-40
Knee	S	Extention-0-bend	0-0-130
crurotalar articulation and Chopart's joint	S	Extention-0-bend	20-0-45
	R	Converting - 0 - turning away	20-0-40

A properly selected illumination must fulfil following requirements:

- maximum contrast between observed features,
- minimum contrast between features, which are not objects of the examination,
- minimum sensibility for changes in the process.

The kind of illuminated object is a very important factor that must also be considered in the course of establishing the type of applied illumination. The most common phenomena observed during the process of illuminating are: absorption of light, reflection, transmission, refraction (partial reflection), dispersion (e.g. rough surfaces) and emission [2], [5], [10], [14], [23], [30].

Cameras in the vision system are most often equipped with integrated illumination in form of LED diodes, placed around the objective. In most cases, this amount of light is sufficient for making a correct inspection. Diodes illuminate the object with impulses of light with the frequency programmed in the memory (light impulses of diodes are giving more lighting than in case of the constant illumination). However, situations in which one should apply the special lighting, adjusted suitably to occurring conditions, are happening. The most frequent mistake is that people do not use all possibilities of machine vision systems. The developed communication with most frequent protocols gives the possibility of large integration with the environment (drivers, implementation devices, etc.). For example: the combination of the system with the barcode reader or with the RFID system gives the possibility of checking the contents of the container (e.g. multi-packs with water) and its accordance with the label [6], [14], [28].

Sensors used in machine vision systems are also important elements.

Machine vision systems have a developed area of equipment and software; this gives them more potential for using them. Sensors gives input data (like results of measurements), unlike detectors that only inform whether the determined condition is fulfilled or not [6], [13-15], [20], [23].

Machine vision systems used in the quality control have many possibilities. The image obtained from a camera is preliminarily processed before the control itself starts.

Possibilities of some vision systems are following [6], [13-15], [23]:

- detection of the image (yes, no),
- summing up objects,
- comparing with the standard and determining the size of the discordance,
- dimensioning (often used in processes of cut, cutting, drilling, threading and other of this type),
- identification of the model in different plains and under different angles,
- monitoring colours (used among others in the food industry),
- identification of the object.
- Exemplary application of machine vision systems [4], [7], [14], [15], [22]:
- examining the correctness of making the intermediate product or the final product,
- identification of objects,
- recognizing,
- reading of 1D, 2D bar codes and ASCII signs,
- summing up objects,
- sizing and measuring,
- sorting.

3 Review of chosen methods of measuring the reach of joint mobility

3.1. Ranges of joints' movements

The correct range of movement of a joint is one of more important factors of the efficiency and the method of measuring it is one of basic methods of assessing the state of the motor organ and a measure of the result of rehabilitation activity. The measurement of the range of mobility in joints is realized with the use of specialist instruments called goniometers. They can be significantly diversified: starting from simple ones, based on the principle of a standard protractor, gravitational protractor, to complicated, electronic instruments, using the phenomenon of the change of the capacity of covers of the condenser depending on the location or change of the resistance of sphygmomanometers. Simple goniometers are sufficient for static measurements of passive ranges of movements in joints. However, when the angle position should be measured in a continuous way, it is necessary to use electronic goniometers. Such situation takes place in measurements of ranges in dynamic conditions, in conditions of motion [3], [14], [15], [27], [29], [32].

The measurement of ranges of movements is established to be relatively not objective. This assumption is connected with the great freedom of the position, in which the measurement is realized (differences can reach even circa 20% of value) or with a relatively big error between particular people conducing measurements. In last years, the SFTR method of measurement and record of results becomes popular, which aims at increasing the scale of objective assessment in the process of measuring the range of movements. Movements in all joints are measured from the neutral zero position and all positions and movements are described in three basic planes with use of the SFTR method [5], [29], [31].

3.2. Methods for measuring the range of mobility

Amongst many universally used methods of measuring the scope of limbs' mobility one should mention among others methods [29]:

- RTG method – a very accurate method, but because of the risk resulting from the radiation, it is not applied in everyday life,
- photographic - suitable for publishing and documentary destinations,
- trigonometrical - great error of measurement, impossibility while examining,
- spherometric measurement - for examining spheroid joints, is held on the surface of a sphere, results are being marked graphically on a cartographic net – lengthy,
- kinematic – is based on establishing temporary reallocations middle of the movement in ponds, difficult to do,
- perimetric - is coming from the method used in ophthalmology,
- outlining - for the application in duction of the wrist and fingers,
- planimetric - goniometry – measurement of the movement only in one plain, most universal in practice.

Conclusions

The developments of digital imaging as well as the new possibilities of digital image analysis allow us to apply these technologies for the analysis of human joints flexibility. Particularly interesting is the ability to accurate measurement of the progress achieved in rehabilitation and treatment of the patient. The currently proposed systems are complex and not too precise which results in discouragement of the medical community to use them. For this reason the development of a reliable and user-friendly method of measurement and analysis seems to be necessary.

Acknowledgment

The article was created within framework of the projects VEGA 1/0872/16 Research of synthetic and biological inspired locomotion of mechatronic systems in rugged terrain.

References

[1] RUSS J. C., The Image Processing Handbook, CRC Press, Wydanie V, 2007,
[2] CHORAŚ R. S., Komputerowa Wizja. Metody interpretacji i identyfikacji obiektów (in Polish), EXIT, Warsaw 2005,
[3] MEYER-BÄSE A.,Pattern recognition for medical imaging, Elsevier Academic Press, 2004,
[4] STĄPOR K., Methods of classification of objects in computer vision (in Polish), PWN, 2011,
[5] SZCZECHOWICZ J., Pomiary kątowe zakresu ruchu : zapisy pomiarów, metoda SFTR, Wyd. Akademia Wychowania Fizycznego im. Bronisława Czecha w Krakowie; Nr 23 - ISBN 83-89121-76-X,
[6] TADEUSIEWICZ R., Vision systems of industrial robot, WNT, Warszawa (in Polish), Warsaw 1996r,
[7] WOŹNICKI J., Podstawowe techniki przetwarzania obrazu (in Polish), Wydawnictwo Komunikacji i Łączności, Warszawa 1996,
[8] ACTON S., RAY N., Biomedical Image Analysis: Tracking, Morgan & Claypool, 2005,
[9] HARTLEY R., ZISSERMAN A., Multiple View Geometry in Computer Vision, 2nd ed. Cambridge University Press, ISBN: 0521540518, 2004,
[10] NAJARIAN K., SPLINTER R., Biomedical Signal and Image Processing, Kayvan Najarian, CRC Press; Wydanie I, 2005,
[11] TADEUSIEWICZ R., OGIELA M., Modern Computational Intelligence Methods for the

Interpretation of Medical Images, Springer, Berlin 2008,
[12] ZALEWSKI A., CEGIEŁKA R., Matlab. Obliczenia numeryczne i ich zastosowanie (in Polish). WNT. Warsaw 1999r,
[13] CYTOWSKI J., GIELECKI J., GOLA A., Cyfrowe przetwarzanie obrazów medycznych. Algorytmy. Technologie. Zastosowania (in Polish), Wydawnictwo EXIT, Warszawa 2008,
[14] SANKOWSKI D., MOSOROV W., STRZECHA K., Processing and image analysis in industrial systems (in Polish), Warsaw 1996r., PWN, 2011,
[15] RANGAYYAN R. M., Biomedical Image Analysis, CRC Press; Edition I, 2004,
[16] DEUTSCHER, J., BLAKE, A., REID, I., Articulated body motion capture by annealed particle filtering, IEEE Int. Conf. on Pattern Recognition, 2000, 126–133,
[17] NAGESH Y., BLEAKLEY C. LENNON J., Wearable Absolute 6 DOF Exercise Training System for Post Stroke Rehabilitation, Proceedings of the Fourth Irish Human Computer Interaction Conference (iHCI 2010) 2-3 September 2010, Dublin, Ireland
[18] SCHMIDT, J., FRITSCH, J., KWOLEK, B., Kernel particle filter for real-time 3D body tracking in monocular color images, IEEE Int. Conf. on Automatic Face and Gesture Rec., 2006,
[19] SIDENBLADH, H., BLACK, M. FLEET, D., Stochastic tracking of 3D human figures using 2D image motion, in: Europen Conference on Computer Vision, 2000,
[20] ROSALES, R., SIDDIQUI, M., ALON, J., SCLAROFF, S., Estimating 3d body pose using uncalibrated cameras, Int. Conf. on Computer Vision and Pattern Recognition, 2001,
[21] SIGAL, L., BHATIA, S., ROTH, S., BLACK, M.J., ISARD, M., Tracking loose-limbed people, IEEE Int. Conf. on Computer Vision and Pattern Recognition, 2004, vol. 1,
[22] HOSKE M. T.,The many faces of industrial Ethernet (in Polish), Control Engineering nr 6 vol. 59, 2003,
[23] POPPE, R., Vision-based human motion analysis: an overview, Computer Vision and Image Understanding 108, 2007,
[24] IVEKOVIC, S., TRUCCO, E., PETILLOT, Y.R., Human body pose estimation with particle swarm optimization, Evolutionary Computation 16 (2008) 509-528,
[25] FANG, YUE G., HROVAT K., SAHGAL V., DALY J., Abnormal cognitive planning and movement smoothness control for a complex shoulder/elbow motor task in stroke survivors, Journal of the Neurological Sciences, vol. 256, pp. 21–29, 2007,
[26] BRAGGE T., HAKKARAINEN M., TARVAINEN M. P., TARKKA I. M., KARJALAINEN P. A., A transportable camera based motion analysis system with application to monitoring of rehabilitation of hand, World Congress on Medical Physics and Biomedical Engineering, September 7 - 12, 2009, Munich, Germany IFMBE Proceedings Volume 25/4, 2010,
[27] Data from the rehabilitation department at the Hospital in Nowa Sol in Poland,
[28] http://www.plcworld.pl/index.php?ak=art&id=12www.technomex.com.pl (2012-12-03),
[29] http://archiwum.czd.pl/index.php?id=692 Department of Pediatric Rehabilitation. The Children,s Memorial Health Institute, Warsaw. (2013-11-02),
[30] http://www.plcworld.pl/index.php?ak=art&id=12www.technomex.com.pl (2013-09-03),
[31] www.karaskov.ČeskýBlog.cz (2013-8-12),
[32] www.kinezytetapia.pl (2012-01-29),
[33] www.Fatcat.agh.edu.pl (2013-06-12).

Review process
Single-blind peer reviewed process by two reviewers.

Acta Mechatronica - International Scientific Journal about Mechatronics
Volume: 1 2016 Issue: 2 Pages: 15-20 ISSN 2453-7306

THE CONTROL OF HOLONOMIC SYSTEM

Tomáš Lipták
Department of Mechatronics, Faculty of Mechanical Engineering, Technical University of Košice, Park Komenského 8, 042 00 Košice, Slovakia, e-mail: tomas.liptak@tuke.sk
Michal Kelemen
Department of Mechatronics, Faculty of Mechanical Engineering, Technical University of Košice, Park Komenského 8, 042 00 Košice, Slovakia, e-mail: michal.kelemen@tuke.sk
Alexander Gmiterko
Department of Mechatronics, Faculty of Mechanical Engineering, Technical University of Košice, Park Komenského 8, 042 00 Košice, Slovakia, e-mail: alexander.gmiterko@tuke.sk
Ivan Virgala
Department of Mechatronics, Faculty of Mechanical Engineering, Technical University of Košice, Park Komenského 8, 042 00 Košice, Slovakia, e-mail: ivan.virgala@tuke.sk
Darina Hroncová
Department of Mechatronics, Faculty of Mechanical Engineering, Technical University of Košice, Park Komenského 8, 042 00 Košice, Slovakia, e-mail: darina.hroncova@tuke.sk

Keywords: double inverted pendulum, Lagrange function, linearization, state space, PID regulator
Abstract: This paper deals with the issue of mathematical modelling of the double inverted pendulum. The paper consists of the determination of mathematical model created via Lagrangian, the linearization of system and the design of linear quadratic regulator. For linear stable system were chosen DC motors placed to joints. Further for these motors were set individual components of PID regulator. The last part of article deals with simulation of double inverted pendulum.

1 Introduction

The study of humanoid robots is currently one of the most exciting research projects. Even if some of those works have already demonstrated very reliable dynamic biped walking (Yamaguchi, Soga, Inoue & Takanishi, 1999; Hirai, Hirose, Haikawa & Takenaka, 1998; Nishiwaki, Sugihara, Kagami, Kanehiro, Inaba & Inoue, 2000), we believe it is still important to understand the mathematical theoretical background of biped locomotion. The locomotion of human body can be considered as the movement of inverted pendulum with certain number of joints, e.g. we can consider human arm as triple inverted pendulum [1].

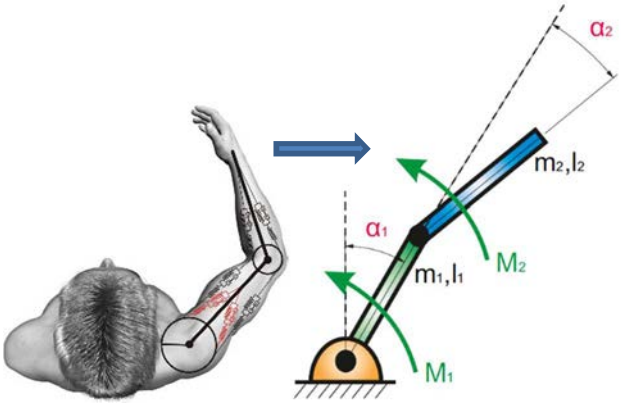

Figure 1 Human arm as double inverted pendulum

An inverted pendulum system is a typically nonlinear, redundancy, uncertainty, strong coupling and natural characteristics of instabilities. All these features make it the ideal model of advanced control theory and typical experiment platform of test control results. There are a number of different kinds of the inverted pendulum systems presenting a variety of control challenges. The most common types are [1]:

- the single inverted pendulum on a cart,
- the double inverted pendulum on a cart,
- the double inverted pendulum with an actuator at the first joint only,
- the double inverted pendulum with an actuator at the second joint only,
- the light weight rotary pendulum and
- other combinations.

In this paper was solved the stability problem of *the double inverted pendulum with actuators at both joints* in the upright position and at joints were used the same DC motors. The pendulum is pivoted at the lower end of inner arm (Figure 1).

The first step to achieve the objective is to understand the dynamics of the system of double inverted pendulum by developing the mathematical modelling of the system. In modelling, we have used Euler-Lagrange formulation to find equation of motion. In the second step, we linearized this non-linear system of double inverted pendulum in the up-up position and builded up its linear

Acta Mechatronica - International Scientific Journal about Mechatronics
Volume: 1 2016 Issue: 2 Pages: 15-20 ISSN 2453-7306

state space model. The linearization is one of the most important issues for control of non-linear systems. In the next step, the stability and controllability criteria showed that the system is unstable but it is controllable.

2 The motion equation of the double inverted pendulum

The position and orientation of the double inverted pendulum in the plane is represented by two *shape variables*–angles $q=(\alpha_1,\alpha_2)$. Then *the configuration space* of pendulum is $Q=G\times M=M=\alpha_1\times\alpha_2$. This configuration space can be visually represented as *a torus* T^2 that arises as combination of two basic building blocks of configuration space, i.e. by combining two circles (Figure 2) [2].

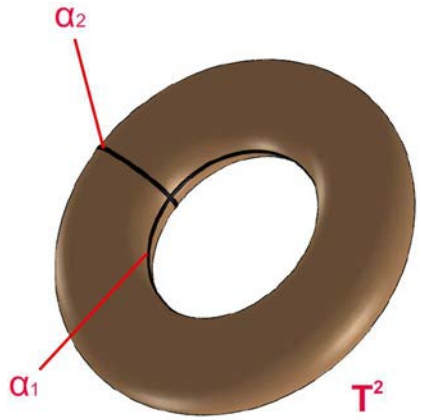

Figure 2 The configuration space of double inverted pendulum

The double inverted pendulum belongs to *holonomic systems*. For holonomic systems apply that their holonomic constraints remove degrees of freedom from a system, reducing the dimensionality of its configuration space. Formally, a holonomic constraint is defined as a (possibly time-varying) constraint function f on the system's configuration space Q. The *zero set* of the function forms the *accessible manifold* of the constrained system, the set of configurations satisfying the constraint [3].

The mathematical model of pendulum was derived using the Euler-Lagrange equation [4]:

$$\frac{d}{dt}\frac{\partial L}{\partial \dot{\alpha}}-\frac{\partial L}{\partial \alpha}=M, \tag{1}$$

where $L=Ek-Ep$ is *Lagrangian*, E_k is *kinetic energy*, E_p is *potential energy* and M is generalized torque produced by actuators placed at joints. The kinetic energy of inverted pendulum has the form:

$$E_{k1}=\frac{1}{6}m_1l_1^2\dot{\alpha}_1^2, \tag{2}$$

$$E_{k2}=\frac{1}{6}m_2l_1^2\dot{\alpha}_1^2+\frac{1}{6}m_2l_2^2\dot{\alpha}_2^2+\frac{1}{3}m_2l_1l_2\dot{\alpha}_1\dot{\alpha}_2\cos(\alpha_1-\alpha_2). \tag{3}$$

The potential energy is defined as:

$$E_{p1}=m_1g\frac{l_1}{2}\cos\alpha_1, \tag{4}$$

$$E_{p2}=m_2g\left(l_1\cos\alpha_1+\frac{l_2}{2}\cos\alpha_2\right). \tag{5}$$

After substituting of individual terms of kinetic and potential energy to Lagrangian and after substituting to equation (1), we get the motion equations of double inverted pendulum:

$$\begin{aligned}&\frac{1}{3}m_1l_1^2\ddot{\alpha}_1+\frac{1}{3}m_2l_1^2\ddot{\alpha}_1+\frac{1}{3}m_2l_1l_2\ddot{\alpha}_2\cos(\alpha_1-\alpha_2)\\&-\frac{1}{3}m_2l_1l_2\dot{\alpha}_2\sin(\alpha_1-\alpha_2)(\dot{\alpha}_1-\dot{\alpha}_2)\\&+\frac{1}{3}m_2l_1l_2\dot{\alpha}_1\dot{\alpha}_2\sin(\alpha_1-\alpha_2)-m_1g\frac{l_1}{2}\sin\alpha_1\\&-m_2gl_1\sin\alpha_1=M_1,\end{aligned} \tag{6}$$

$$\begin{aligned}&\frac{1}{3}m_2l_2^2\ddot{\alpha}_2+\frac{1}{3}m_2l_1l_2\ddot{\alpha}_1\cos(\alpha_1-\alpha_2)\\&-\frac{1}{3}m_2l_1l_2\dot{\alpha}_1\sin(\alpha_1-\alpha_2)(\dot{\alpha}_1-\dot{\alpha}_2)\\&-\frac{1}{3}m_2l_1l_2\dot{\alpha}_1\dot{\alpha}_2\sin(\alpha_1-\alpha_2)-m_2g\frac{l_2}{2}\sin\alpha_2\\&=M_2.\end{aligned} \tag{7}$$

3 The linearisation of inverted pendulum

The double inverse pendulum is described by two non-linear equations of motion. We need to linearize this non-linear system in operating point closely to steady state. Assuming small deviations we can use the following angle approximations [5]:

$$\begin{aligned}&\alpha_1\approx\alpha_2\approx0,\\&\cos\alpha_1\approx\cos\alpha_2\approx1,\\&\sin\alpha_1\approx\alpha_1,\\&\sin\alpha_2\approx\alpha_2,\\&\alpha_1-\alpha_2\approx0,\\&\cos(\alpha_1-\alpha_2)\approx1,\\&\sin(\alpha_1-\alpha_2)\approx\alpha_1-\alpha_2,\\&\dot{\alpha}_1^2\approx\dot{\alpha}_2^2\approx0.\end{aligned} \tag{8}$$

After application of previous equations, motion equations take the form:

Acta Mechatronica - International Scientific Journal about Mechatronics
Volume: 1 2016 Issue: 2 Pages: 15-20 ISSN 2453-7306

$$\frac{1}{3}l_1^2\ddot{\alpha}_1(m_1+m_2)+\frac{1}{3}m_2l_1l_2\ddot{\alpha}_2 - \alpha_1\left(m_1g\frac{l_1}{2}+m_2gl_1\right)=M_1, \quad (9)$$

$$\frac{1}{3}m_2l_2^2\ddot{\alpha}_2+\frac{1}{3}m_2l_1l_2\ddot{\alpha}_1-m_2g\frac{l_2}{2}\alpha_2=M_2. \quad (10)$$

Linearized motion equations (9) and (10) we rewrite to the form of state equations [5]:

$$\dot{\mathbf{x}}=\mathbf{A}\mathbf{x}+\mathbf{B}\mathbf{u}, \quad \mathbf{y}=\mathbf{C}\mathbf{x}+\mathbf{D}\mathbf{u}. \quad (11)$$

After substituting the values of parameters for the inverted pendulum:

- m_1=0,5kg,
- m_2=0,5kg,
- l_1=1m,
- l_2=1m,

form of matrices is as follows:

$$\mathbf{A}=\begin{bmatrix} 0 & 1 & 0 & 0 \\ 44{,}145 & 0 & -14{,}715 & 0 \\ 0 & 0 & 0 & 1 \\ -44{,}145 & 0 & 29{,}43 & 0 \end{bmatrix},$$

$$\mathbf{B}=\begin{bmatrix} 0 & 0 \\ 6 & -6 \\ 0 & 0 \\ -6 & 12 \end{bmatrix}, \mathbf{C}=\begin{bmatrix} 1 & 0 & 0 & 0 \\ 0 & 0 & 1 & 0 \end{bmatrix}, \quad (12)$$

$$\mathbf{D}=\begin{bmatrix} 0 & 0 \\ 0 & 0 \end{bmatrix}, \mathbf{u}=\begin{bmatrix} M_1 \\ M_2 \end{bmatrix}.$$

4 The linear quadratic regulator

A state-space design approach is well suited to the control of multiple outputs as we have here. This problem can be solved using full-state feedback. The schematic of this type of control system is shown below (Figure 3) where ***K*** is a *matrix of control gains*.

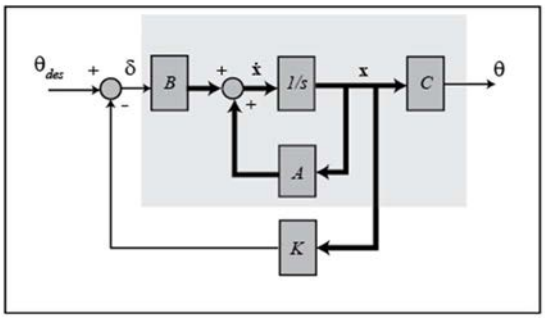

Figure 3 The schematic of full-state feedback control system [6]

The first step in designing a full-state feedback controller is to determine the open-loop poles of the system. The open-loop poles for inverted pendulum we can solve using command in programme MATLAB [6]:

- poles=eig(A),

where we work with matrix ***A***. These poles can be obtained also by solving of the characteristic equation of *transfer function.*

Based on the above mentioned matrices from equation (12) we will make the transfer functions using *Laplace transform* assuming zero initial conditions. Laplace transform is yet another operational tool for solving constant coefficients linear differential equations (Figure 4). The process of solution consists of three main steps:

- the given "hard" problem is transformed into a "simple" equation,
- this simple equation is solved by purely algebraic manipulations,
- the solution of the simple equation is transformed back to obtain the solution of the given problem.

In this way the Laplace transformation reduces the problem of solving a differential equation to an algebraic problem. The third step is made easier by tables, whose role is similar to that of integral tables in integration [7].

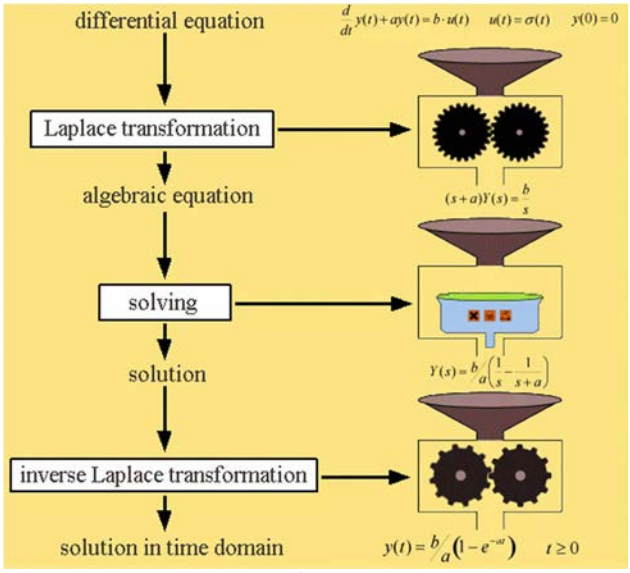

Figure 4 The schematic of Laplace and inverse Laplace transform [8]

The transfer functions of inverted pendulum created using the Laplace transform express relation between outputs α_1, α_2 and inputs M_1, M_2 and their form is:

Acta Mechatronica - International Scientific Journal about Mechatronics
Volume: 1 2016 Issue: 2 Pages: 15-20 ISSN 2453-7306

THE CONTROL OF HOLONOMIC SYSTEM

Tomáš Lipták; Michal Kelemen; Alexander Gmiterko; Ivan Virgala; Darina Hroncová

$$\frac{\alpha_1}{M_1}=\frac{6s^2-2{,}665.10^{-15}s-88{,}29}{s^4+2{,}665.10^{-15}s^3-73{,}57s^2-3{,}126.10^{-13}s+649{,}6}$$
$$\frac{\alpha_2}{M_1}=\frac{-6s^2+1{,}588.10^{-22}s+1{,}213.10^{-13}}{s^4+2{,}665.10^{-15}s^3-73{,}57s^2-3{,}126.10^{-13}s+649{,}6} \quad (13)$$
$$\frac{\alpha_1}{M_2}=\frac{-6s^2-2{,}528.10^{-14}}{s^4+2{,}665.10^{-15}s^3-73{,}57s^2-3{,}126.10^{-13}s+649{,}6}$$
$$\frac{\alpha_2}{M_2}=\frac{12s^2+1{,}066.10^{-14}s-264{,}9}{s^4+2{,}665.10^{-15}s^3-73{,}57s^2-3{,}126.10^{-13}s+649{,}6}$$

The poles for inverted pendulum are:

- p_1=-7,9571,
- p_2=7,9571,
- p_3=-3,2031,
- p_4=3,2031.

The two poles of the open control system are located in the right half-plane of complex variable s, from it follows that the double inverted pendulum is unstable system (Figure 5).

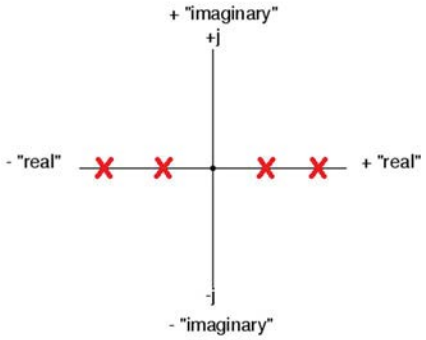

Figure 5 Two poles of the open control system

On the following figure (Figure 6) is course of the angular rotation of joints unstable inverted pendulum α_1 and α_2 when inputs M_1 and M_2 are *1Nm*.

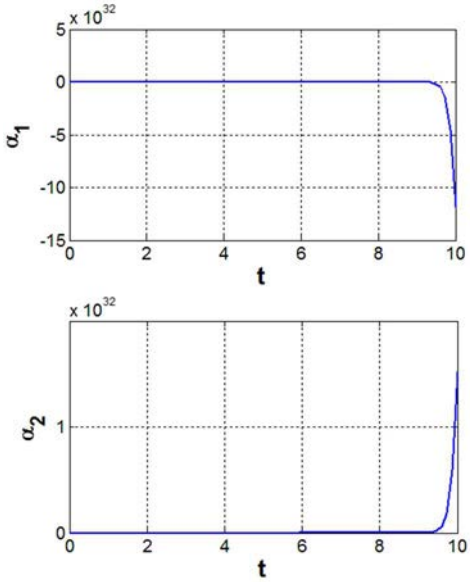

Figure 6 The course of the angular rotation of joints of unstable inverted pendulum α_1 and α_2

Before we design our controller, we will first verify that the system is *controllable*. Satisfaction of this property means that we can drive the state of the system anywhere we like in finite time (under the physical constraints of the system). For the system to be completely state controllable, the controllability matrix *CO* must have rank *n* where the rank of a matrix is the number of independent rows (or columns). The number *n* corresponds to the number of state variables of the system. The controllability of system was established using commands [6]:

- *CO=ctrb (transfer_functions),*
- *controllability=rank(CO).*

Inverted pendulum is described by four state variables and the rank of controllability matrix is four, that is, it follows that *the system is controllable*.

We will use *the linear quadratic regulation* method for determining our state-feedback control gain matrix ***K***.

Na jej výpočet opäť využijeme MATLAB pomocou príkazov [6]:

- *Q=C'*C,*
- *R=[1 0;0 1],*
- *K=lqr(A,B,Q,R).*

After determining state-feedback control gain matrix:

$$\mathbf{K}=\begin{bmatrix}14{,}0666 & 2{,}8816 & 1{,}1348 & 1{,}0010\\ -3{,}1814 & 0{,}1161 & 4{,}8456 & 0{,}9957\end{bmatrix} \quad (14)$$

We can assemble the transfer functions of stable inverse pendulum:

$$\frac{\alpha_1}{M_1}=\frac{6s^2+35{,}85s+86{,}15}{s^4+22{,}54s^3+180{,}4s^2+598{,}7s+708}$$
$$\frac{\alpha_2}{M_1}=\frac{-6s^2-4{,}179s+114{,}5}{s^4+22{,}54s^3+180{,}4s^2+598{,}7s+708} \quad (15)$$
$$\frac{\alpha_1}{M_2}=\frac{-6s^2-36{,}04-40{,}85}{s^4+22{,}54s^3+180{,}4s^2+598{,}7s+708}$$
$$\frac{\alpha_2}{M_2}=\frac{12s^2+103{,}7s+241{,}5}{s^4+22{,}54s^3+180{,}4s^2+598{,}7s+708}$$

To achieve a vertical position up was added another block *PID controller* to the block diagram. A proportional–integral–derivative controller is a control loop feedback mechanism (controller) commonly used in industrial control systems. A PID controller continuously calculates an *error value* as the difference between a desired setpoint and a measured process variable. The controller attempts to minimize the error over time by adjustment of a *control variable*, such as the position of a control valve, a damper, or the power supplied to a heating element, to a new value determined by a weighted sum:

$$u(t)=K_p e(t)+K_i\int_0^t e(\tau)d\tau+K_d\frac{de(t)}{dt} \quad (16)$$

where K_p, K_i and K_d all non-negative, denote the coefficients for the proportional, integral, and derivative

Acta Mechatronica - International Scientific Journal about Mechatronics
Volume: 1 2016 Issue: 2 Pages: 15-20 ISSN 2453-7306

terms, respectively (sometimes denoted P, I, and D). In this model:

- *P* accounts for present values of the error. For example, if the error is large and positive, the control output will also be large and positive.
- *I* accounts for past values of the error. For example, if the current output is not sufficiently strong, error will accumulate over time, and the controller will respond by applying a stronger action.
- *D* accounts for possible future values of the error, based on its current rate of change.

As a PID controller relies only on the measured process variable, not on knowledge of the underlying process, it is broadly applicable. By tuning the three parameters of the model, a PID controller can deal with specific process requirements. The response of the controller can be described in terms of its responsiveness to an error, the degree to which the system overshoots a setpoint, and the degree of any system oscillation. The use of the PID algorithm does not guarantee optimal control of the system or even its stability.

Some applications may require using only one or two terms to provide the appropriate system control. This is achieved by setting the other parameters to zero. A PID controller will be called a PI, PD, P or I controller in the absence of the respective control actions. PI controllers are fairly common, since derivative action is sensitive to measurement noise, whereas the absence of an integral term may prevent the system from reaching its target value [9].

The individual components P, I and D were automatically generated after running the button *Tune*, by which was designed the most suitable controller for controlling of inverted pendulum. From the transfer functions we constructed the course of the angular rotation α_1 and α_2 of the joints (Figure 7), where we can see that *the system is stable*.

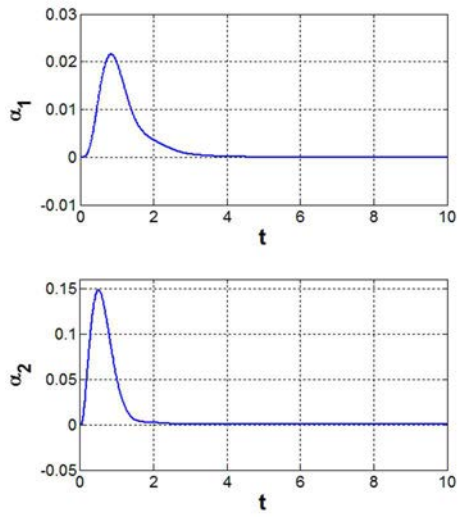

Figure 7 The course of the angular rotation of joints of stable inverted pendulum α_1 and α_2

To the block diagram (Figure 9) were finally added also DC motors with power supply 6V and their parameters are [10]:

- L=0,000121H,
- k_m=0,00449Nm/A,
- k_b=0,00448Vs/rad,
- J=2,18.10^{-5}kgm^2,
- B=9,0946Nms/rad,
- R=2,22Ω.

Using Laplace transform we created the transfer function for DC motors:

$$\frac{\alpha_{1,2}}{U} = \frac{0{,}00449}{2{,}637.10^{-9}s^2 + 0{,}001148843s + 27{,}19}. \quad (17)$$

The process of generating values of PID controller was again realized. The course the angular rotation of joints of inverted pendulum, when on input to block diagram is already placed power supply of DC motors, we can see in the figure below (Figure 8).

The simulations were carried out with zero initial conditions and deviations in individual courses were caused only due to gravity.

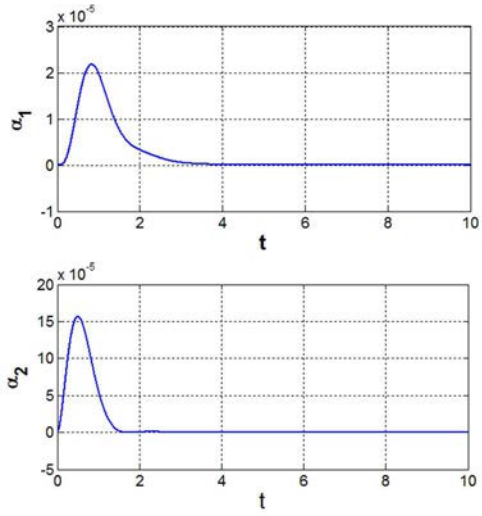

Figure 8 The course of the angular rotation of joints of stable inverted pendulum α1 and α2 in connection with DC motors

Conclusion

The article deals with the issue of stabilization of the double inverted pendulum. After the determination of the mathematical model of pendulum using Euler-Lagrange equation, we were able to linearize system. From the mathematical model transformed into the state space through MATLAB were verify the stability and controllability of system. After the determination state-feedback control gain matrix K using linear quadratic control method and individual components of PID controller were created block diagrams, which were then also simulated.

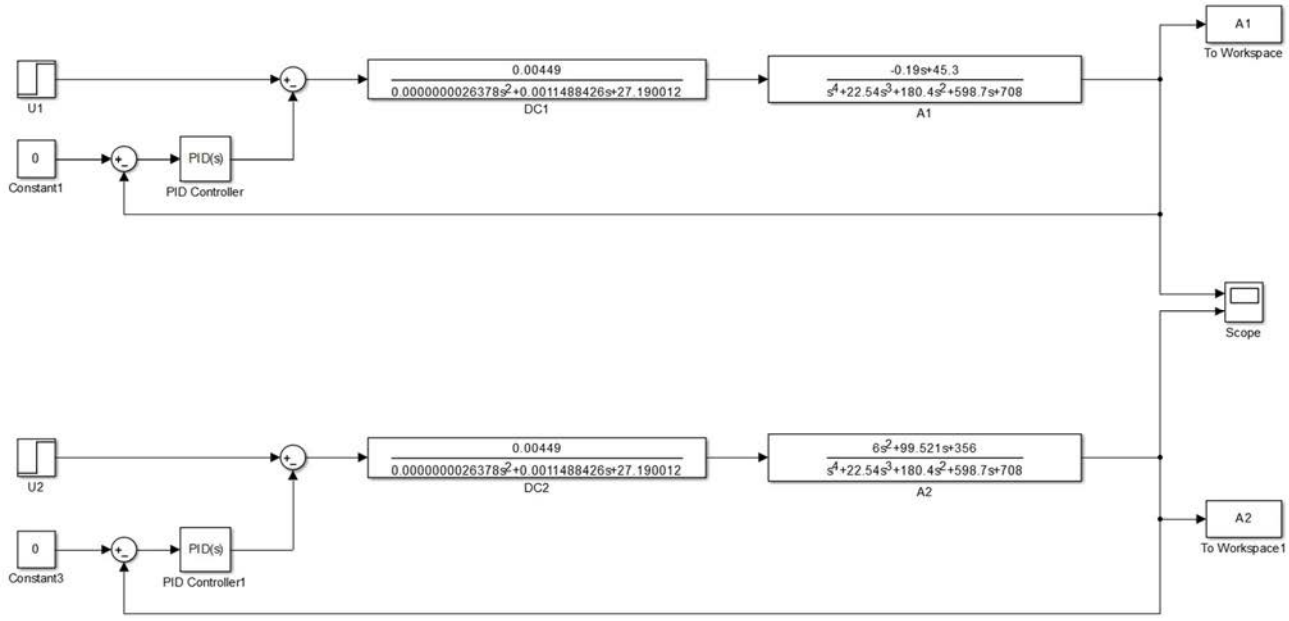

Figure 9 The complete block diagram of the double inverted pendulum expressed using a complex variables

Acknowledgement
The work has been accomplished under the research projects No. VEGA 1/0872/16 "Research of synthetic and biological inspired locomotion of mechatronic systems in rugged terrain".

References

[1] SHAH, N., YEOLEKAR, M.: Pole Placement Approach for Controlling Double Inverted Pendulum. India: University of Ahmedabad, 2013.
[2] OSTROWSKI, J.: The Mechanics and Control of Undulatory Robotic Locomotion. The dissertation thesis. California Institute of Technology Pasadena, September 19, 1995. pp. 137.
[3] HATTON Ross L., CHOSET Howie, An Introduction to Geometric Mechanics and Differential Geometry, December 6, 2011.
[4] SHAMMAS, E.: Generalized Motion Planning for Underactuated Mechanical Systems. The dissertation thesis. Pennsylvania: Carnegie Mellon University Pittsburgh, March 20, 2006. pp. 167.
[5] JORDAN, A.: Linearization of non-linear state equation. Bulletin of the Polish Academy of Sciences Technical Science. Vol.54. pp. 63-73.
[6] http://ctms.engin.umich.edu/CTMS/index.php?example=InvertedPendulum&section=ControlStateSpace(cit. 1.2.2016).
[7] http://faculty.atu.edu/mfinan/4243/Laplace.pdf(cit. 10.2.2016).
[8] http://www.atp.rub.de/DynLAB/dynlabmodules/Examples/Laplacetransform/Rickeracke.html(cit. 18.2.2016).
[9] http://www.rpi.edu/dept/chem-eng/WWW/faculty/bequette/simulink.pdf(cit. 1.3.2016).
[10] http://www.maxonmotor.com/maxon/view/catalog/(cit. 1.3.2016).

Review process
Single-blind peer reviewed process by two reviewers.

Acta Mechatronica - International Scientific Journal about Mechatronics
Volume: 1 2016 Issue: 2 Pages: 21-25 ISSN 2453-7306

OPTIMAL CONTROL OF MANIPULATOR GRIP POSITION TO MOVE FLAT OBJECTS

Andrej Ivanovich Abramov
Kalashnikov Izhevsk State Technical University, Department of Mechatronic Systems, Studencheskaya 7, 426069, Izhevsk, Russia, hitech1015@yandex.ru
Ivan Vasilevich Abramov
Kalashnikov Izhevsk State Technical University, Department of Mechatronic Systems, Studencheskaya 7, 426069, Izhevsk, Russia, abramov@istu.ru
Pavol Božek
Department of Control and Information Systems, Institute of Applied Informatics, Automation and Mechatronics, Faculty of Materials Science and Technology, Slovak University of Technology, 917 24 Trnava, Slovak Republic, pavol.bozek@stuba.sk
Timur Mazitov
Kalashnikov Izhevsk State Technical University, Department of Mechatronic Systems, Studencheskaya 7, 426069, Izhevsk, Russia, rymit1991@yandex.ru
Alexey Palmov
Kalashnikov Izhevsk State Technical University, Department of Mechatronic Systems, Studencheskaya 7, 426069, Izhevsk, Russia, palmov-a@yandex.ru

Keywords: Contour, Moments, Hu Moments, Part Orientation, Flat Parts
Abstract: The methodology to explicitly define the flat object orientation in 2D space is proposed. A number of experiments with modelled data have been carried out, as a result, the developed methodology has been successful tested and importance of precise contour extraction of the object has been confirmed. The methodology obtained can be applied during the automation of processes of moving flat parts, sorting out of parts by shape and other similar operations.

1 Introduction

In the process of industrial enterprise automation, flat objects (parts) are traditionally represented in 2D form in a large number of technological operations. Contour extraction is one of such methods. The application of contour analysis makes it possible to define the most important parameters of objects (area, center of mass, etc.). Moment characteristics of contour and moment invariants calculated on their basis, which are the most important tools for image identification due to their insensibility to orientation, scale, viewing angle and other measurements are widely spread [1], [2]. However, the use of such contour features and characteristics does not allow explicitly defining a part orientation on a plane. When representing an object as a contour it is necessary to precisely extract the part outline – to separate the object and background. The incorrect contour definition results in the change of its characteristics and identification errors.

2 Contour extraction

Contour is an object outline, which separates it from the background or other objects. The contour analysis allows finding, describing, storing and comparing objects. A number of coding methods are used to store and describe a contour. Freeman code, in which the aggregate of pixels in the object outline is represented in the form of vectors with definite length and direction, is widely applied [3].

Limitations imposed onto the application area of contour analysis are mainly connected with problems of contour extraction on images: due to the same brightness with the background the object sometimes does not have a vivid outline or can be blurred resulting in the impossibility of contour extraction; object overlapping results in improper contour extraction and mismatch with the object outline.

There are a number of algorithms of image transformation to extract contours [4], [5]:

- Threshold transformation
- Canny operator
- Sobel operator
- Laplace operator
- Prewitt operator
- Roberts operator

Each of the algorithms has its own advantages and disadvantages, the correct selection and combination of different filters and algorithms when processing images

Acta Mechatronica - International Scientific Journal about Mechatronics
Volume: 1 2016 Issue: 2 Pages: 21-25 ISSN 2453-7306

and extracting contours play an important role [6], [7], [8].

The application of contour analysis allows significantly decreasing computational complexity as it gives the possibility to move from 2D image processing to contour processing based on the comparison of their characteristics.

3 Contour characteristics

Moment is a contour characteristic calculated through the integration (summation) of all contour pixels. The moment (k, s) is defined by the following formula [1]:

$$M_{ks} = \int_{-\infty}^{\infty}\int_{-\infty}^{\infty} m^k n^s x(m,n)dmdn, \quad k,s = 0,1,\ldots \quad (1)$$

The moments found by the above formula depend on coordinate system, therefore, they do not allow defining a turned figure, and they are also sensible to scale – they do not allow comparing contours with the same shapes but different sizes.

To provide the invariability to image scaling, first it is necessary to normalize the moments – bring them to one length (operation of contour equalization). Such moments are called central.

Computation of central moments [1]:

$$\mu_{ks} = \int_{-\infty}^{\infty}\int_{-\infty}^{\infty}(m-\bar{m})^k(n-\bar{n})^s x(m,n)dmdn, \quad k,s = 0.1,\ldots, \quad (2)$$

where: $\bar{m} = \frac{M_{10}}{M_{00}}$, $\bar{n} = \frac{M_{01}}{M_{00}}$ — center of mass defining the object position.

The characteristics invariant to image turning are defined with the help of central moments.

The computation of normalized central moments:

$$\eta_{ks} = \frac{\mu_{ks}}{M_{00}^{(\frac{k+s}{2}+1)}}. \quad (3)$$

Certain combinations of the moments give the possibility to make the following 7 transformations of moment characteristics, which are invariant to shifts, turns, expansions and compressions (scaling) and where initially proposed by M. K. Hu [1].

Moment invariants by Hu:

$$Hu_1 = \eta_{02} + \eta_{20}; \quad (4)$$

$$Hu_2 = (\eta_{02} + \eta_{20})^2 + 4\eta_{11}{}^2; \quad (5)$$

$$Hu_3 = (\eta_{30} + \eta_{12})^2 + (3\eta_{21} - \eta_{03})^2; \quad (6)$$

$$Hu_4 = (\eta_{30} + \eta_{12})^2 + (\eta_{21} - \eta_{03})^2 \quad (7)$$

$$Hu_5 = (\eta_{30} + 3\eta_{12})(\eta_{30} + \eta_{12})[(\eta_{30} + \eta_{12})^2 - 3(\eta_{21} - \eta_{03})^2] + (3\eta_{21} - \eta_{03})(\eta_{21} + \eta_{03})[3(\eta_{30} + \eta_{12})^2 - (\eta_{21} + \eta_{03})^2]; \quad (8)$$

$$Hu_6 = (\eta_{02} + \eta_{20})[(\eta_{30} + \eta_{12})^2 - (\eta_{21} + \eta_{03})^2] + 4\eta_{11}(\eta_{30} - \eta_{12})(\eta_{21} + \eta_{03}); \quad (9)$$

$$Hu_7 = (3\eta_{21} + \eta_{03})(\eta_{30} + \eta_{12})[(\eta_{30} + \eta_{12})^2 - 3(\eta_{21} + \eta_{03})^2] - (\eta_{30} - 3\eta_{12})(\eta_{21} + \eta_{03})[3(\eta_{30} + \eta_{12})^2 - (\eta_{21} + \eta_{03})^2]. \quad (10)$$

Contour comparison of two objects is brought to the correlation of corresponding Hu moments. The correlation is defined by one of the following formulas:

$$Kor_1(\alpha,\beta) = \sum_{i=1\ldots7}\left|\frac{1}{H_i^\alpha} - \frac{1}{H_i^\beta}\right| \text{ or} \quad (11)$$

$$Kor_2(\alpha,\beta) = \sum_{i=1\ldots7}\left|H_i^\alpha - H_i^\beta\right| \text{ or} \quad (12)$$

$$Kor_3(\alpha,\beta) = \sum_{i=1\ldots7}\left|\frac{H_i^\alpha - H_i^\beta}{H_i^\alpha}\right|, \quad (13)$$

where $H_i^\alpha = |Hu_i^\alpha| * \log Hu_i^\alpha$, $H_i^\beta = |Hu_i^\beta| * \log Hu_i^\beta$.

Another important characteristic of a contour is inertia moments [6]. The inertia moment is a scalar quantity characterizing the inertia degree in rotation about an axis. The quantity J_a is the figure inertia moment about a fixed axis ("axial moment of inertia") equaled to the total of products of mass of all *n* material points of the system and the squares of their distances to the axis [9]:

$$J_a = \int r^2 dm, \quad (14)$$

where dm is mass of body element and *r* is distance from the element to axis *a*.

The main central axes of inertia pass through the center of figure mass – axes relating to which the product of inertia equals zero:

$$J_{xy} = J_{xz} = 0,$$

where $J_{xy} = \int xydm$, $J_{xz} = \int xzdm$.

Let us assume that *u* and *v* are the main. Then:

$$J_{uv} = \frac{J_x - J_y}{2} sin2a + J_{yz} cos2a = 0. \quad (15)$$

Hence:

$$tg\ 2a = \frac{2J_{yz}}{J_x - J_y}. \quad (16)$$

This equation defines the position of main axes of inertia of the figure in the given point relating to the initial coordinate axes. However, in this formula *a* changes from 0 up to 180^0 that does not allow explicitly defining the contour orientation. The algorithm based on the additional contour extraction was proposed to solve this problem.

4 Algorithm for defining contour orientation

The algorithm is applied on the preliminarily extracted, by correlation coefficient of Hu moments, the

Acta Mechatronica - International Scientific Journal about Mechatronics
Volume: 1 2016 Issue: 2 Pages: 21-25 ISSN 2453-7306

pair of similar contours, one of which is the reference standard.

The algorithm comprises two parts: teaching by the given reference standard and orientation computation relating to the reference standard.

Teaching:

1. Divide the contour into 2 parts along the small axis of inertia.
2. Select one of the contours obtained.
3. Define moments for the contour selected.
4. Define the orientation as a vector from the part center of mass to the center of mass of the contour obtained at the second stage.

Definition of relative orientation:

1. Divide the contour into 2 parts along the small axis of inertia.
2. Define moments for the contour selected.
3. Find the most similar contour by correlation coefficient of Hu moments extracted at the teaching stage.
4. Construct the vector from the part center of mass to the center of mass of the contour obtained at the third stage. The vector obtained characterizes the part orientation.
5. The difference between vector angles of the reference standard and contour investigated defines the object turning angle relating to the reference standard position.

The proposed methodology allows explicitly defining the flat object orientation for further manipulations with it.

5 Finding the optimal position of manipulator grip

When moving parts, the manipulator performs linear and rotational motions which result in dynamic loads that need to be minimized. Moments of inertia create the main additional load. Centrifugal moments of inertia relating to the main central axes equal 0, therefore, it is necessary to fix the part in such a way as to align the part rotation axis and main axes of inertia. The grip for parts needs to be positioned on the manipulator following the same rule. The main central axes of inertia of the part (a) and manipulator grip (b) are demonstrated in Figure 1 [10, 11].

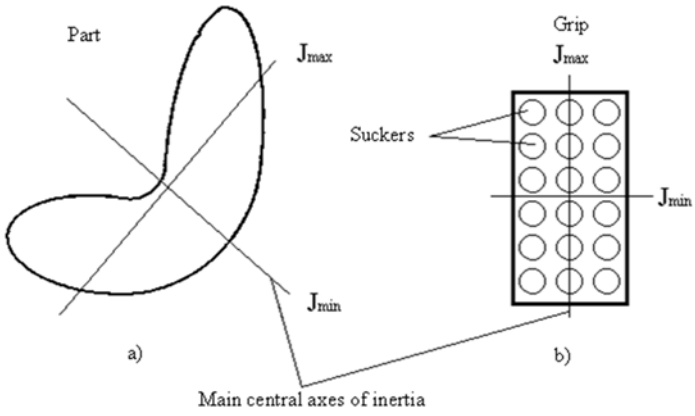

Figure 1 Main central axes of inertia of the part and manipulator grip

The manipulator grip for moving flat objects is the structure on which vacuum suckers are fastened to fix objects.

The alignment of central axes of inertia of manipulator grip and part with the rotation axis allows minimizing dynamic loads.

6 Experiment results

The samples of flat parts, demonstrated in Figure 2, were generated to test the algorithm obtained.

Figure 2 Trial samples of flat parts

Samples A,B,C imitate typical parts of furniture manufacturing, sample D – more complicated part.

Fig. 3 demonstrates the trial sample processed following the algorithm obtained. The extracted features are vividly illustrated.

Acta Mechatronica - International Scientific Journal about Mechatronics
Volume: 1 2016 Issue: 2 Pages: 21-25 ISSN 2453-7306

OPTIMAL CONTROL OF MANIPULATOR GRIP POSITION TO MOVE FLAT OBJECTS

Andrej Ivanovich Abramov; Ivan Vasilevich Abramov; Pavol Božek; Timur Mazitov; Alexey Palmov

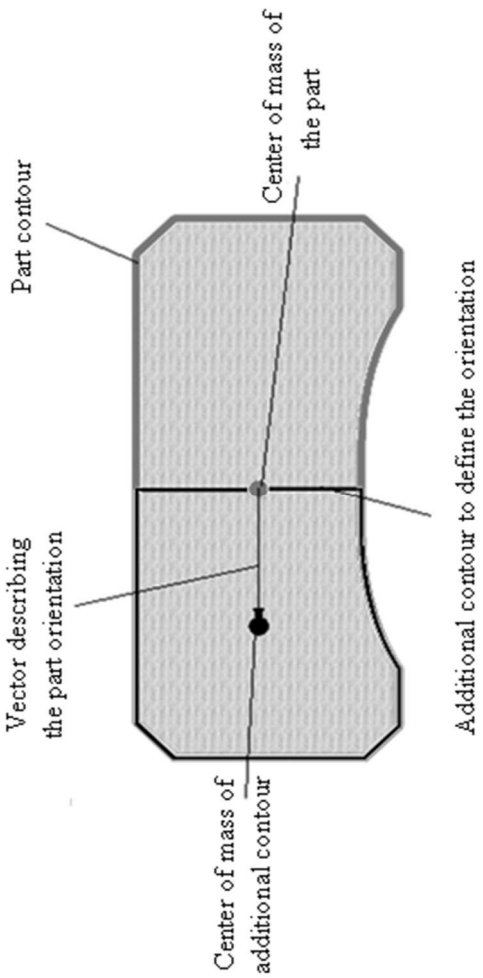

Figure 3 Processed trial sample

The part contour and additional contour are indicated in the figure, which allow making an orienting vector going through the centers of mass of the part and additional contour.

To evaluate the accuracy of orientation definition, the trial samples were turned around 45^0, 90^0, 180^0, 200^0 and 270^0. During the experiment the actual angles were compared, around which the parts were turned, and the angles calculated following the algorithm. The results are given in the table.

Table Angles calculated following the algorithm

Part / Angle	A	B	C	D
45	45.01	45.04	44.84	45.23
90	90.08	90.00	90.00	90.15
180	180.08	180.00	180.00	180.15
200	200.22	200.02	199.93	199.96
270	270.64	270.09	270.00	270.00

The maximum deviation was 0.2396^0. The deviation is explained by slight distortions in images during turning as in the modeled data not the part contour but the whole image rotated. The average time spent on computation of the part orientation on the image of 1800x1600 pixels was 0.231 second.

The developed algorithm was also tested on the actual sample. The experiment results are demonstrated in Fig. 4.

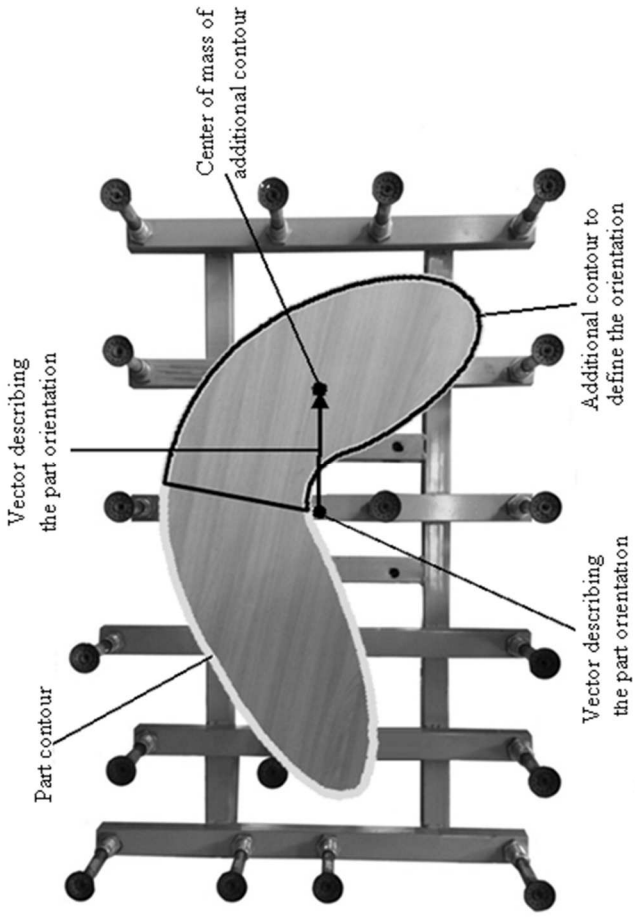

Figure 4 Actual sample

The figure demonstrates the part and its characteristics found according to the methodology developed that allow defining the orientation. The part is positioned on the manipulator grip.

Conclusions

The methodology based on extracting an additional contour in the object investigated is proposed. It allows explicitly defining the orientation of a flat object in 2D space. A number of experiments with modeled data were carried out. As a result, it was revealed that precise contour extraction is the most important condition as all the computed characteristics depend on it. The precise contour extraction is reached with the help of the correct selection and combination of different filters and

algorithms when processing images. The methodology obtained can be applied during the automation of processes of moving flat parts, sorting out of parts by shape and other similar operations.

Acknowledgement
The contribution is sponsored by VEGA MŠ SR No. 1/0367/15 prepared project „Research and development of a new autonomous system for checking a trajectory of a robot“.

References

[1] HUANG, Z., LENG, J.: Analysis of Hu's moment invariants on image scaling and rotation, *Computer Engineering and Technology (ICCET)*, 2nd International Conference on, Vol. 7, pp. 476-478, 2010.
[2] FLUSSER, J., SUK, T.: Pattern recognition by affine moment invariants, *Pattern recognition*, Vol. 26, No. 1 pp. 167-174, 1993.
[3] FREEMAN, H.: Computer processing of line-drawing images, *ACM Computing Surveys (CSUR)*, Vol. 6, No. 1 pp. 57-97, 1974.
[4] KHRYASCHEV, D.A.: *On one method of contour extraction on digital images*, Bulletin of Astrakhan State Technical University. Series: Control, computer engineering and informatics. No. 2, 2010.
[5] SOIFER, V.A.: Computer processing of images. Part 2. Methods and algorithms, *Soros educational journal*, No. 3, P. 110-121, 1996.
[6] MAINI, R., AGGARWAL, H.: Study and comparison of various image edge detection, *International journal of image processing (IJIP)*, Vol. 3, No. 1, P. 1-11, 2009.

Review process
Single-blind peer reviewed process by two reviewers.

Acta Mechatronica - International Scientific Journal about Mechatronics
Volume: 1 2016 Issue: 2 Pages: 27-30 ISSN 2453-7306

THREE AXIS LINEAR PORTAL MANIPULATOR

Milan Lörinc
VVU ZTS, a.s., Južná trieda 95, Kosice, Slovak Republic, milan.lorinc@ztsvvu.eu

Keywords: mechatronics, manipulator, actuator, sensor
Abstract: Three axis portal manipulator is nornally designed with four portal comception. This paper describes special type of three axis manipulator with only two portals. Designed manipulator are designed for educational purpose and practical training for students. RC servos are used as acutators for moving of all axis. Resistive sensors are used for sensing of movement in *x, y* axis.Rotary encoder is used for *z* axis movement sensing.

1 Introduction

Development of manipulators has been started from 70^{ties} years of last century and it is coupled with substitution of human hand work. New technologies enable rapidly development of new generations of manipulators which are applied in various area of industry as metallurgy hard manipulator, automotive industry manipulator, montage manipulator, medical manipulator, space flight manipulators etc.

Characteristic attribute of linear manipulators is linear movement in all axes. Very often are used acronym cartesian or portal robots. Applications of these types of manipulators are mainly in manipulation with objects, mounting process and they are often also called as pick & place robots.

Solved manipulator has been developed as didactic aid for educational purposes. Almost all these type of manipulator has four pillars and it can be as problem for inserting of handled objects etc. Our solution (Figure 1) has only two pillars, so that is better for insetting of handled objects.

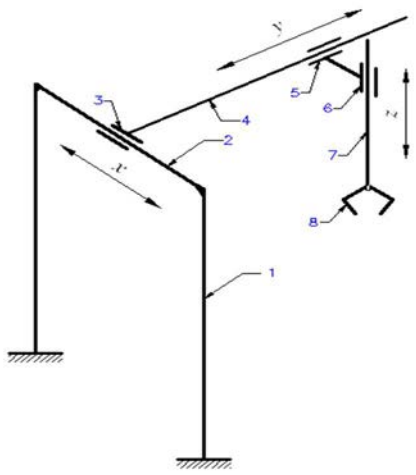

Figure 1 Conception of two pillar cartesian manipulator

It consist (fig. 1) of two pillars (1), x traverse (2) with guiding (3) connected to y traverse with guiding (5) connected to z guiding (6) with steering pivot (7) in axis z. End-effector (8) is connected to steering pivot (7).

This conception (Figure 2) is ambitious, because the main problem is stiffness and stability of all parts, which can be as source of oscillating of end-effector.

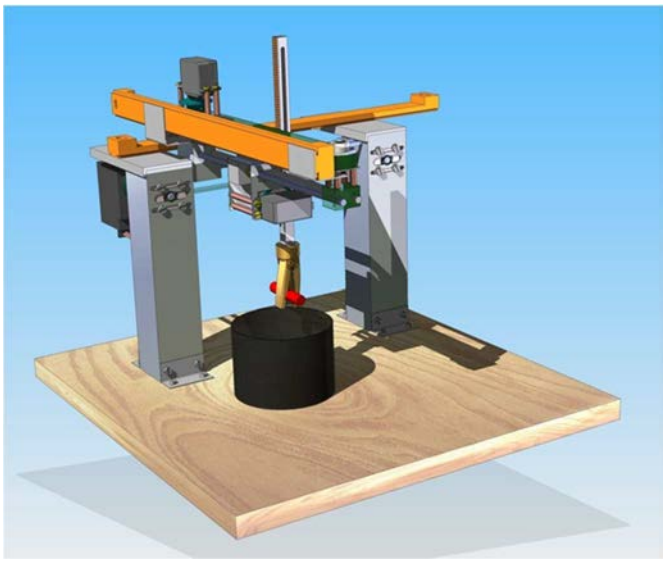

Figure 2 3D model of conception of two pillar cartesian manipulator

2 Construction of two pillar manipulator

Robotic servos have been used as drive units for generation of motion in all axis and they converts electrical energy to mechanical works. These types of servos are controlled with pulse with modulation signal. The servos are modified to continual rotation. It means that desired value of velocity rotation is defined via using of duty cycle.

THREE AXIS LINEAR PORTAL MANIPULATOR
Milan Lörinc

Position resistive sensors are used for measuring of actual position in all axes and this information is used for feedback for position control. These types of sensor are not preferred but several last years' research and development in this are growing up and new type of resistive elements and wiper have been introduced. Also this type of new sensor has very long life up to 50 million cycles.

Used servos are rotational actuators and it is necessary to convert rotation to linear motion. Toothed belts have been used for this conversion (Figure 3)

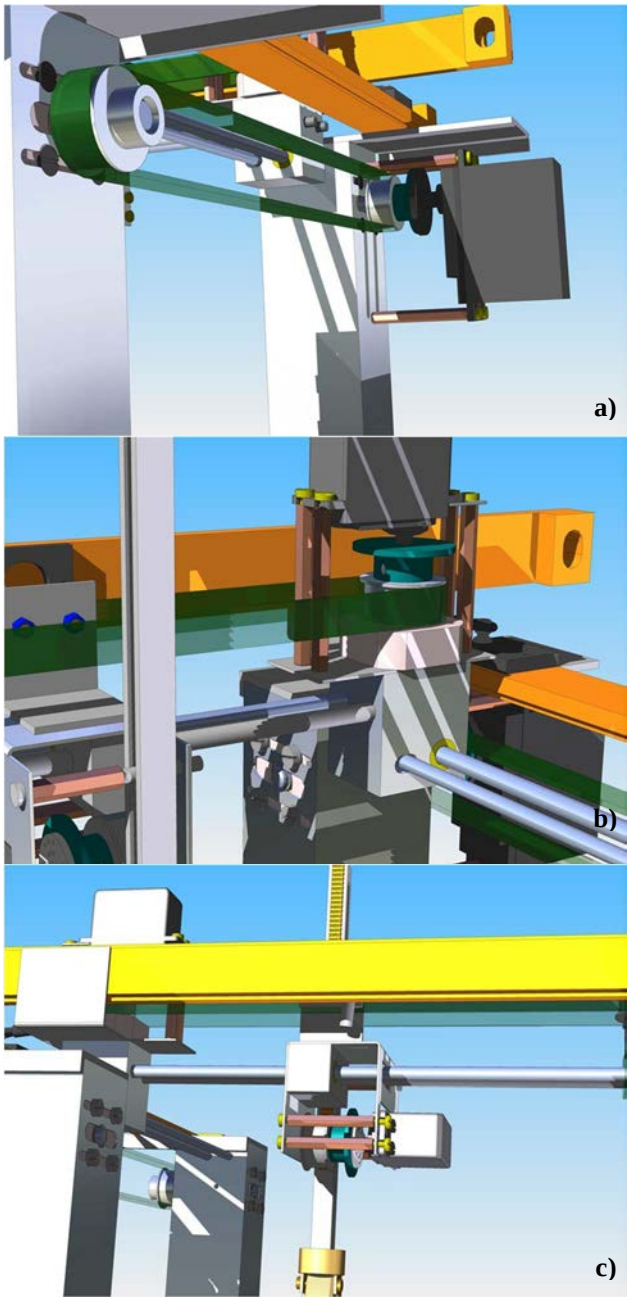

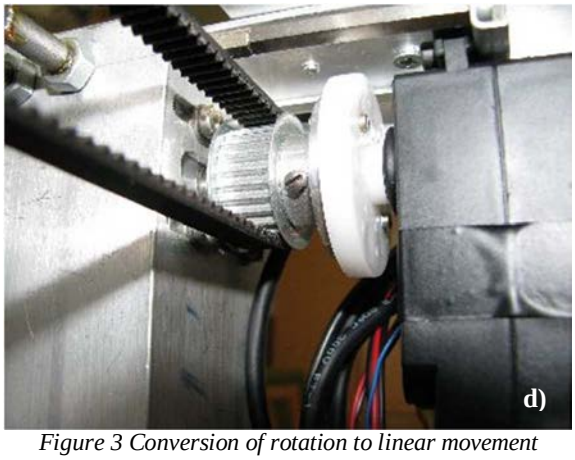

Figure 3 Conversion of rotation to linear movement

Main advantage of toothed belts is power transmission without belt creeping but tightening mechanism is necessary for right function of belts. Tightening mechanism causes additional load to construction of manipulators. This additional loading has to be considered into design and calculation of manipulator for both X and Y axis.

Z axis (Figure 4) has been more complicated. Beam for Z axis with endeffector cannot be carried via using the same way as X and Y axis.

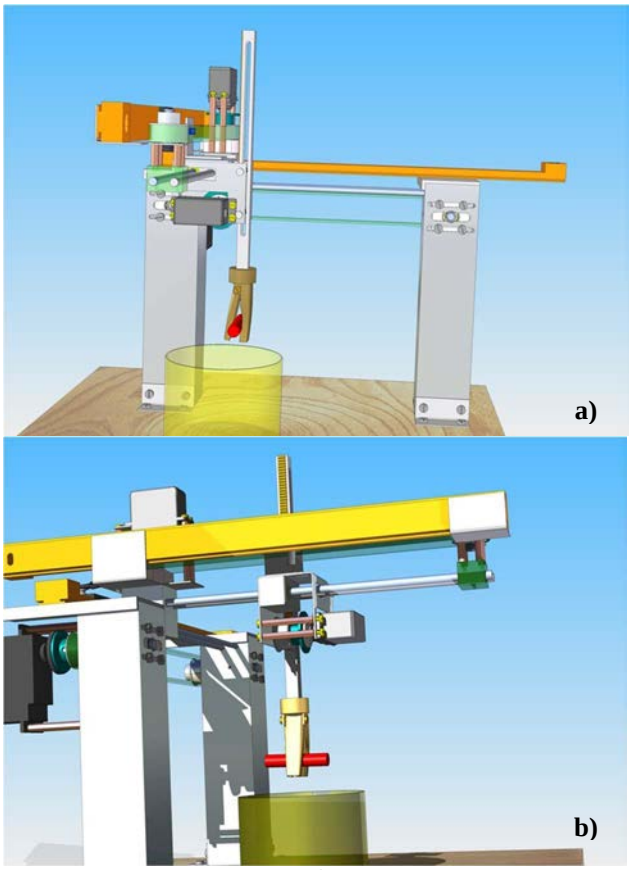

Figure 4 Design of Z axis movement

Beam for Z axis has attached piece of tightened toothed belt. Belt pulley is attached to output horn of servo. Position of Z axis can be counted via using of optical encoder rotational sensor connected to servo. Final design of axis movements defines the manipulation work-space of end-effector (Figure 5). Simplicity of manipulator construction also enables the simple programming than joint manipulator with large number of degree of freedom.

All sensors and actuators can be connected to microcontroller or data acquisition card. This manipulator is designed as didactic tool, and students can train data acquisition of signals and feedback controlling. Also results obtained from inverse kinematic can be included into program. Other special task is the solving of dynamic effects for manipulating with hanged weights. That is the similar problem like weight manipulating via using of crane.

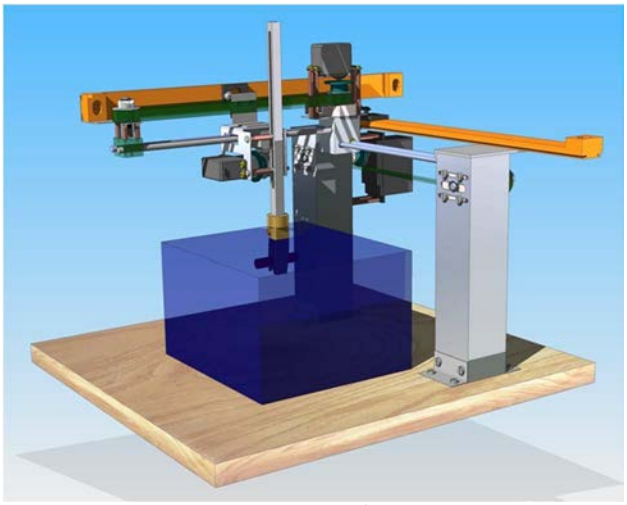

Figure 5 Work-space of manipulator

3 Conclusion

This concept of manipulator helps to understand various problems from several areas of science. Stiffness of construction is another problem, which can has impact to control process. Also used mechanisms have any disadvantage as tooth backlash, backlash of bearings, friction forces etc. All these effect cannot be neglected in design of control [1]-[15].

References

[1] STANKOVSKI, S., TARJAN, L., SKRINJAR, D., OSTOJIC, G.: *'Using a Didactic Manipulator in Mechatronics and Industrial Engineering Courses '*, In: IEEE Transactions on Education. Volume:53 Issue:4, p. 572 - 579, 2010.

[2] KELEMENOVÁ, T., FRANKOVSKÝ, P., VIRGALA, I., MIKOVÁ, Ľ., KELEMEN, M.: Machines for inspection of pipes, *Acta Mechatronica*, Vol. 1, No. 1, 1-7. 2016.

[3] CORREA, J. C., RAMÍREZ. J.A., TABORDA, E. A..: *'Implementation of a Laboratory for the Study of Robot Manipulators'*,Paper No. IMECE2010-39136, pp. 23-30; 8 pages, Volume 6: Engineering Education and Professional Development Vancouver, British Columbia, Canada, November 12–18, 2010.

[4] GMITERKO, A., VIRGALA, I., MIKOVÁ, Ľ., FRANKOVSKÝ, P., KELEMENOVÁ, T., KELEMEN, M.: *'Machines for in-pipe inspection'*, In: Journal of Automation and Control. Vol. 3, no. 3 (2015), p. 79-82. 2015.

[5] VAGAŠ, M., SUKOP, M., BALÁŽ, V., SEMJON, J.: *'The calibration issues of 3D vision system by using two 2D camera sensors'*.In: International Scientific Herald. Vol. 3, no. 2 (2012), p. 234-237. 2012

[6] GMITERKO, A., VIRGALA, I.,- MIKOVÁ, Ľ., FRANKOVSKÝ, P., KELEMENOVÁ, T., KELEMEN, M.: Machines for in-pipe inspection. *In: 'Journal of Automation and Control'*, Vol. 3, no. 3 (2015), p. 79-82

[7] SUKOP, M., HAJDUK, M., BALÁŽ, V., SEMJON, J., VAGAŠ, M.: Increasing degree of automation of production systems based on intelligent manipulation, *Acta Mechanica Slovaca*, Vol. 15 (2011), pp. 58–63. 2011.

[8] KELEMEN, M., VIRGALA, I., MIKOVÁ, Ľ., FRANKOVSKÝ, P.: Experimental Identification of Linear Actuator Properties, *Acta Mechanica Slovaca*, Vol. 19, No 1, (2015), pp. 42–47. 2015.

[9] HAJDUK, M., JÁNOŠ, R., SUKOP, M., TULEJA, P., VARGA, J.: Trends of developments in industrial robotics, *AT&P Journal.*, No. 5, pp. 17–19, 2012.

[10] YUM, Y. J., HWANG, H. S., KELEMEN, M., MAXIM, V., and FRANKOVSKÝ, P.: In-pipe micromachine locomotion via the inertial stepping principle, *Journal of Mechanical Science and Technology* 28 (8) (2014), 3237-3247. 2014.

[11] SUKOP, M., JÁNOŠ, R.: Proposal of internal positioning system for mobile robotics *'Transfer of innovation'*, No 30, 2014, pp. 114-115, 2014.

[12] DUCHOŇ, F., HUBINSKÝ, P., HANZEL, J., BABINEC, A., TÖLGYESSY, M.: Intelligent Vehicles as the Robotic Applications, *Procedia Engineering*, Volume 48, 2012, Pages 105–114. 2012.

[13] KONIAR, D., HARGAŠ, L., ŠTOFAN, S.: Segmentation of Motion Regions for Biomechanical Systems, *Procedia Engineering*, Volume 48, 2012, Pages 304–311. 2012.

[14] BOŽEK, P., TURYGIN, Y.: Measurement of the operating parameters and numerical analysis of the mechanical subsystem, *Measurement Science Review*, Vol. 14, No. 4, pp. 198-203, 2014.

[15] ABRAMOV, I. V., NIKITIN, Y. R., ABRAMOV, A. I., SOSNOVICH, E. V., BOŽEK, P.: Control and Diagnostic Model of Brushless DC Motor, *Journal of Electrical Engineering*. Volume 65, Issue 5, Pages 277–282, 2014.

Review process
Single-blind peer reviewed process by two reviewers.